This is to certify that the

thesis entitled

THE EFFECTS OF RELATIVE HUMIDITY ON THE PERMEATION OF
TOLUENE THROUGH POLY-(ETHYLENE VINYL ALCOHOL) (EVAL)

presented by

STEPHEN SING-TOH TAN

has been accepted towards fulfillment
of the requirements for

M. S. degree in Chemical Engineering

K Jayaraman
Major professor

Date 9/22/86

O-7639

MSU is an Affirmative Action/Equal Opportunity Institution

THE EFFECTS OF RELATIVE HUMIDITY ON THE PERMEATION
OF TOLUENE THROUGH
POLY-(ETHYLENE VINYL ALCOHOL) (EVAL)

BY

STEPHEN SING-TOH TAN

A THESIS

Submitted to
Michigan State University
in partial fulfillment of the requirements
for the degree of

MASTER OF SCIENCE

Department of Chemical Engineering

1986

ABSTRACT

THE EFFECTS OF RELATIVE HUMIDITY ON THE PERMEATION OF TOLUENE THROUGH POLY-(ETHYLENE VINYL ALCOHOL) (EVAL)

BY

STEPHEN S.T. TAN

The effects of water vapor on the barrier properties of EVAL with respect to Toluene have been studied in this work. An attempt has been made to relate the permeability data to physical and mechanical properties. The glass transition temperature of the film was measured at varying relative humidity using a Differential Scanning Calorimeter. Stress relaxation experiments were carried out in the Instron tensile tester afer each permeation runs.

At 75 %RH and above, permeation was detected at a measurable level, but at 50 %RH, no permeation was detected. This observation maybe related to a decrease in glass transition temperature due to the plasticization effects of toluene and water vapor on the EVAL semi-crystalline matrix. This proposed explanation is supported by the relaxation times.

ACKNOWLEDGMENTS

I would like to express my appreciation to the following people for their help in this study.

Dr. K. Jayaraman for his guidance throughout my research.

Dr. J. Giacin from the School of Packaging for his professional advice, continuous support, guidance and use of his laboratory.

The Mass Transfer Group: Ruben Hernandez, Larry Baner, Kenny Liu, Susan Mohney, Lynn Dixon, Heidi Hoojjat, and Terri Bonfiglio for sharing their friendship, knowledge and skills.

The Michigan Molecular Institute for allowing me to conduct DSC experiments at their facility and to Karl Dunkirk for assisting me.

I also acknowledge Cryovac Co. for providing film samples and financial support for this study.

I am further grateful to Dr. Donald Anderson, Chairperson of Chemical Engineering Dept., for providing teaching assistantships during this study.

TABLE OF CONTENTS

Page

LIST OF TABLES

LIST OF FIGURES

Nomenclature

a_{ϵ}	shear strain shift factor
a_D	relative diffusivity, D_1/D_0
A_D	minimum "hole" size required to accommodate the diffusing molecule
B_D	proportionality constant
B	empirical constant of order of unity
c	concentration of the permeant in the polymer
D	diffusion coefficient, in^2/min
D_T	thermodynamic diffusion coefficient
D_0	pre-exponential diffusion factor
E_R	relaxation modulus at a single time
E_S	Young's modulus
f	fractional free volume
$f_{0\epsilon}$	fractional free volume at zero strain
f_i	free volume fraction in the medium specified by the subscript

H	relaxation spectrum
H_1	first approximation of relaxation spectrum
H_2	second approximation of relaxation spectrum
δH_s	heat of solution
L	thickness of the film
$\delta M/\delta t$	transmission rate at steady state
p'	pressure at one face of the membrane
$\overline{P}$	Permeability coefficient, g-structure/m^2 day-ppm
Q_s	steady state flow rate per unit area
R	universal gas constant
S	Solubility
S_o	limiting solubility constant
t	time
$t^{1/2}$	time required for Q to achieve $Q_s/2$
T	absolute temperature, °K
T_g	glass transition temperature, °K
v	local volume-fraction concentration of the penetrant

v_F^{o}	standard reference for fractional free volume at a reference temperature and pressure
V	observed specific volume
V_l^{o}	volume of the liquid state
V	critical local hole free volume

Greek Letters

α_G	thermal expansion coefficient at the glassy state
β	interaction parameter (same as δf)
β_F	coefficient of compressibility of free volume
β_ϵ	total compressibility coefficient of the polymer
γ	gamma function
σ_s	shear stress
μ	Poisson's ratio
τ	relaxation time
θ	lag time required for the film to approach steady state diffusion
ϵ_s	tensile strain
ϵ	diffusion effect between permeant-polymer interaction during transient and steady state

Subscripts

∞	steady state
1	polymer
2	diluent

INTRODUCTION

The effects of water vapor on the physical and mechanical properties of polymer films have been studied extensively in the literature, especially the plasticization effect on hydrophilic films. As for the effects of organic vapor on barrier films, there is a lack of complete understanding of the interaction of organic vapor on high barrier films. This deficiency is further compounded by the paucity of studies conducted on the simultaneous effects of organic vapor and water vapor on the barrier properties of polymer films.

This study reports on the effects of organic and water vapor on ethylene vinyl alcohol copolymer (EVAL), a high barrier polymer film, as determined by mass transfer methods and mechanical properties measurements. Toluene is the organic vapor used in this study. Due to insufficient time and availability of film , a complete study on the mutual effects of both permeants as well as the effects of the individual permeants on EVAL was not considered. Rather, this study concentrated on the physical and mechanical effects by the individual permeants on the polymer film and on the mass transfer rate of toluene through EVAL films preconditioned at specified relative humidity levels.

The mass transfer method applied was the quasi-isostatic permeation procedure and the data obtained was the transmission rate profile of toluene through EVAL films preconditioned to a given relative humidity. The solubility of water vapor in the EVAL films was also determined as a function of relative humidity.

The physical properties measured were the glass transition temperature and specific volume changes with varying relative humidity only. The mechanical property evaluated was the stress relaxation, which was determined following exposure to varying relative humidity and organic vapor concentrations. The equipment included the Differential Scanning Calorimeter, Thermal Mechanical Analyzer and Instron tensile tester respectively for each property.

By studying the physical and mechanical properties, the phenomena of mass transfer can be better understood. The sorption of water vapor by the film samples results in changes in physical and mechanical properties, thereby affecting the mass transfer of toluene through the film samples. Hence, the correlation between the mechanical properties and the mass transfer properties can then be better identified.

LITERATURE REVIEW

The physical properties of barrier polymer films (e.g. Saran, HDPE) have been studied extensively with super-critical gases (e.g. oxygen). Salame (1984) has studied the permeation of supercritical gases through glassy polymers. Vrentas and Duda (1985) have studied the permeation of both organic vapors and supercritical gases through polymers at elevated temperatures. Both authors related the concentration and temperature dependence by means of a free volume parmameter, which is a function of the motion of chain ends, the motion of side ends, and the motion of the main chain. This study is aimed at relating the concentration dependence of organic vapor and relative humidity with physical and mechanical properties measurements below the glass transition temperature.

I. Glass transition temperature

A fundamental property of polymers is the glass transition temperature Tg. It is defined as a point, or narrow region on a temperature scale, where the thermal expansion coefficient undergoes a discontinuity and below which the configurational rearrangement of polymer chain backbones are extremely slow (Ferry, 1970). As temperature increases through Tg from glass to liquid state, both the intermolecular distances and the packing factor concurrently increase to provide a total change in fractional free volume through the glass transition. At temperatures greater than Tg, the Brownian motion in a polymeric liquid or soft solid is rapid. A lowering of the temperature would result in a decreased Brownian motion of the molecular chains thereby reducing the free volume in the polymeric liquid.

Tg values reported in the literature are based on volumetric measurements using experimental temperature response patterns. Temperatures are raised or lowered continuously at a slow rate or varied intermittently with pauses on the order of an hour, and the time sequences between measurement varied. These practices of varying the rate allow the free volume to reach equilibrium (Ferry, 1970). As a result, values of Tg from different laboratories frequently fail to agree, thus fractional free volume values calculated also vary. Kovacs (1964), has done extensive experiments on obtaining Tg, and recommends a 3 minute conventional time interval for measuring Tg.

II. Physical Properties Measurements

II-A. Mass Transfer Methods

Permeation is defined as the diffusion of gases or liquids through an essentially continuous film or container (ANS, 1979). In 1939, Barrer related the permeability P, the diffusion coefficient D, and the solubility S in an expression:

$$\overline{P} = D\ S \qquad (1)$$

Functionally, $\overline{P}$ describes the steady-state rate of transmission of molecules through a barrier, D describes the rate of molecules advancing, and S describes the film absorbing the molecules (DeLassus, 1985).

II-A.1. Diffusion

In 1959, Cohen and Turnbull showed that for a liquid composed of identical molecules, a probabilistic fractional free volume can be determined. In their study, they defined the free volume as the volume within the packing array of a molecule minus the volume of the molecule itself. This is similar to the definition stated earlier.

Fujita in 1961 extended the Cohen and Turnbull theory to a two-component mixture. He related the average free volume per unit of volume of the system to the thermodynamic diffusion coefficient D_T, as given by the expression:

$$D_T = RTA_D \exp(-B_D /f) \qquad (2)$$

where R is the universal gas constant and T is the absolute temperature. A_D is a function of the "hole" corresponding to the minimum size required for a given diluent molecule to permit a "considerable" displacement into the polymer, and B_D is a proportionality constant. f is the average fractional free volume of the system. A_D and B_D are considered to be independent of temperature and penetrant concentration, but f should be a function of both.

On the basis of theory advanced by Cohen and Turnbull, Vrentas, Duda and Ling (1985) presented a generalized version of the free-volume theory for the self-diffusion process in polymer solutions that can be applied at all temperatures. The expression proposed for D_1, the solute self-diffusion coefficient in a polymer-penetrant mixture,

$$D_1 = D_O \exp\{(E/RT)\}\exp(-\gamma V_1 /V_f) \qquad (3)$$

where D_O defines the pre-exponential factor and E is the activation energy per mole. The term γ, the overlap factor,accounts for the fact that the same free volume is available to more than one molecule. V_1 is the critical local hole free volume required for a molecule of solute to jump to a new position, and V_f is the average hole free volume per molecule in the liquid.

Stern and Fang (1972) presented a study on the effects of high pressure on gas permeability coefficients. The study was related to a modified Fujita's free-volume theory to account for the pressure effects. The extended equation is similar to equation 5 and is given by

$$D = RTA_D \exp [- B_D / (v_F^o + \sigma v) \qquad (4)$$

where v_F^o is the standard reference for the fractional free volume at some reference temperature and pressure, σ is the concentration coefficient, and v is the local volume-fraction concentration of the penetrant in the membrane. The study showed that an increase in the penetrant pressure causes two opposing free volume effects: (a) concentration of the penetrant dissolved in the membrane increased, thereby increasing the free volume, and (b) the hydrostatic pressure on the membrane is also increased, thus causing a decrease in the free volume.

Choy et al (1984) and Peterlin (1974) modified Fujita's free volume theory to account for the concentration dependence of the free volume. The modified expression is given as

$$D = D_o \exp[\phi c]$$

$$D_o = \exp (-B/f) \qquad (5)$$

$$\phi = B \delta f/f^2$$

where D_o is the limiting diffusion coefficient and B is a constant characteristic of the permeant-membrane system, which increases rapidly with the size of the permeant. δf is the effectiveness of the permeant molecule for increasing the free volume of the polymer and c is the concentration of the permeant in the polymer. The coefficient ϕ is directly proportional to the difference of fractional free volume of the components and is inversely proportional to the square of the free volume of the polymer.

Baner (1986) modified Choy's equation to account for the transient state region of the diffusion and sorption process. The equation also takes into consideration the interaction of permeant with the polymer at steady state. The proportionality factor (ϕ) was expressed as:

$$\phi = B (\beta + \epsilon)/f \qquad (6)$$

where β is the interaction parameter (same as δf above). ϵ accounts for the different effect between permeant-polymer interaction during transient and steady state diffusion processes, and f_o is a constant describing the fractional free volume of the polymer at zero vapor concentration (Hernandez, 1985). B and f_o are independent of the permeant concentration.

Kulkarni and Mashelkar (1983) introduced an altered free volume model of the form for polymer solutions, protein solutions, polymeric gels and blends of polymeric melts

$$\ln \frac{1}{a_D} = \frac{f_1(0,T)}{B_D} + \frac{(f_1(0,T)^2}{B_D B(T)} \left\{ \frac{1}{\phi_2} \right\} \quad (7)$$

where a_D is the relative diffusivity, D_2/D_O. D_2 and D_O are the diffusivity of the diluent and of the pure polymer component respectively. f_1 is the free volume fraction in the medium specified by the subscripts, at composition ϕ and temperature T. B_D is the minimum hole size required to accommodate the diffusing molecule. B is the value of the property of the pure component of the block copolymer and is the volume fraction for the species denoted by the ϕ subscripts. The subscripts 1 and 2 refer to the polymer and diluent respectively. The equation can be applied only for diffusivity in the pure polymer and can be used to correlate diffusivity data.

II-A.2. Solubility

The majority of sorption studies described in the literature are performed by measuring the weight differences of the non-interacting adsorbant, absorbed onto the polymer sample. Knowing the molecular structure of the adsorbant, the free volume can be quantitated. However, the interpretation of the obtained results is difficult because of the possibility of dual-mode and multi-layer absorption kinetics due to polymer-adsorbant interaction (Michaels et. al., 1963).

Crank and Park (1951) showed that a constant diffusion coefficient produces the Fickian shape of the sorption-$(\text{time})^{1/2}$ plot. When the equilibrium concentration of sorbed penetrant in polymer is plotted versus the square root of time, a curve that is linear in the region of small values of $t^{1/2}$ and concave against the abscissa in the region of large $t^{1/2}$ values is obtained. The rate of desorption is initially at a faster rate than sorption. At later time, the rate of desorption is relatively slow such that the sorption and desorption curves intersect. These anomalies were attributed to two possible causes; (a) variable surface concentration of permeant, and (b) diffusion coefficient values dependent on the history of the diffusion process.

Petropoulos (1984) described the anomalous sorption kinetics in polymer-penetrant systems as having a common physical origin, namely relatively slow penetrant-induced polymer molecular relaxations. The author proposed that the accommodation of penetrant molecules within the polymer matrix at T < Tg is effected in part by local "elastic" swelling response and partly by a "viscous" swelling response. Effect of a variable surface concentration is well established experimentally, whereas no comparable evidence is available for the diffusion coefficient dependence of history.

The diffusion and sorption theories described in this literature review are only valid in the Fickian region of diffusion. Fickian diffusion is a function of concentration and temperature and not time (Fujita et. al., 1959). Alfrey et al (1966) differentiated Fickian diffusion into two situations based on polymer chain relaxation rates and diffusion rates:(Hernandez, 1984)

1. Rate of diffusion in the system is much less than that of relaxation of the polymer chain segments. The system is controlled by the diffusion coefficient. Here the diffusion coefficient may depend on the concentration of the permeant in the polymer for the specific permeant-polymer system.

2. Relaxation process is much slower than the diffusion rate. This is an apparent Fickian process and the kinetics can be reduced to only the velocity of the advancing front of the diffusant in addition to the equilibrium swelling factor.

II-A.3. Methods of Determination

The diffusion coefficient can be determined from the experimental lag time, obtained from permeability studies by (Barrer, 1939)

$$\theta = L^2/6D \qquad (8)$$

where L is the thickness of the film and θ is the lag time required for the film to approach steady state diffusion.

The lag time method has several drawbacks which limit its effectiveness (Ziegel et. al., 1969). For example, a pressure differential between the low and high pressure sides of a film may result in distortion of the polymer film. A constant concentration gradient requires that the concentration of gas in the receiver remains negligible compared to that of the reservoir. The experimental apparatus should be leak-proof. Ziegel et. al. (1969) proposed in their studies a modification of the conventional lag time method. Here, a continuous removal of the penetrant from the low pressure surface of the membrane by a carrier gas to a detector was employed and ensured that a constant penetrant driving force concentration be maintained. The steady-state transmission rate Q_s per unit area (Q/tA) obeys the relation

$$Q/tA = \overline{P}p'/L \qquad (9)$$

where $\overline{P}$ is the permeability coefficient, p' is the pressure at the high concentration surface of the membrane, Q is the quantity penetrated through the membrane, t is the time, and A is the area of the membrane. The diffusion coefficient is given as

$$D = L^2/(7.199t^{1/2}) \qquad (\ 10\ )$$

where $t_{1/2}$ is obtained graphically from the volume flow rate $(\delta M/\delta t)$ Q versus t curve, when Q is equal to $Q_s/2$.

The solubility coefficient can be calculated from permeation experiments using the measured transmission at steady-state rate, $(\delta M/\delta t)_\infty$, and the diffusivity lag time, D_{LAG}.

$$S = (\delta M/\delta t)/D \qquad (\ 11\ )$$

DeLassus (1985) described two equations used in calculating the diffusion coefficient from permeability experiments. The first equation :

$$D = 0.176\ L^2\ (\text{SLOPE})/(\delta M/\delta t)_\infty \qquad (\ 12\ )$$

where D is the diffusion coefficient, "SLOPE" is the slope of the transient region of permeation when the measured transmission rate is plotted versus time, L is the film thickness, and $(\delta M/\delta t)_\infty$ is the steady state rate (Pasternak et. al., 1970) of transmission. The second equation is Equation 13, as given before by Ziegel et al. (1969).

These relationships were derived from equations described by Barrer (1941), who assumed that both D and S are independent of concentration throughout the duration of the mass transport and sorption processes. As the test proceeds, no vapor/polymer interaction must occur (Zobel, 1982).

The temperature dependence of solubility S is expressed as

$$S = S_o \exp[-\delta H_s / RT] \qquad (13)$$

where S_o is the limiting solubility constant and δH_s is the heat of solution. For easily condensable vapors, S decreases with increasing temperature (Rogers et. al., 1956).

III. Thermal Expansion Methods

The thermal expansion coefficient is related to the specific volume and temperature through the equation

$$V = V_o (1 + \alpha T) \qquad (14)$$

where V and V_o are the observed and the hypothetical specific volume obtained at $T = 0^\circ K$ and α is the thermal expansion coefficient. The volume specified and the expansion coefficient calculated can be in the liquid or glassy state. The thermal expansion coefficient determined from equation 17 may be substituted into an equation developed by Simha and Boyer for fractional free volume

$$f = [V - V_l^o (1 + \alpha_G T)] / V \qquad (15)$$

where α_G is the thermal expansion coefficient of the glassy states. V_l^o is the volume of the liquid state at $T = 0^o K$ obtained by linear extrapolation of the Volume-Temperature function from above Tg.

IV. Mechanical Properties

IV-A. Stress Relaxation

The phenomenon of chemical stress relaxation has been studied extensively with thermoplastic and cross-linked amorphous polymers above and below Tg, as well as, with semi-crystalline polymers. The response of polymers in general to external stress is partly elastic and partly viscous in nature. This viscoelastic behavior is due to interactions of the external stress with the molecular chains, which tend to rearrange into conformations of lower energy (Kaufman and Falcetta, 1977).

The theory of stress analysis in solid bodies for linearly elastic bodies subjected to infinitesimal strains obeys Hooke's law

$$\sigma_s = E_s \epsilon_s \qquad (18)$$

where σ_s is the stress, ϵ_s is the strain and E_s is the Young's modulus, which is a measure of stiffness or resistance to deformation (or shear stress to strain) and is a function of temperature. For nonideally elastic substances, the modulus is a function of time and to some extent, a function of the method of measurement (Ferry, 1970).

Smith (1962) reported that the small-deformation nonlinear creep behavior of some plastics can be represented by an equation in which the time and stress effects are separated. For plastic samples subjected to a fixed extension and stress measured as a function of time, the modulus calculated is defined as the stress relaxation modulus $E_R(t)$. Four well defined regions of viscoelastic behavior exist (Tobolsky, 1956) : (a) a low-temperature glassy region (b) a transition region of elastoviscous behavior (c) a quasi-static "rubbery" plateau region and (d) a liquid flow region. Each of this regions can be categorized by taking a cross section of the modulus-time curve at some fixed relaxation time τ, which is a measure of the rate at which stress decays (Rodriguez, 1982).

Viscoelastic data at one temperature can be transformed to another temperature by a time-temperature superposition principle. This principle is a multiplicative transformation, that is, a horizontal shifting of curves of relaxation times (τ) along the axis of $E_R(t)$ versus log (t) by a uniform shift factor log a_T, such as Equation 2, rewritten to account for the free volume.

$$\log a_T = -(B/2.303 f_o)(T-T_o) \,/\{(f_o/\alpha_f) + T - T_o)\} \qquad (19)$$

where α_f is the thermal coefficient of free volume relative to total volume, T_o is the arbitrary reference temperature, and f_o is the fractional free volume at an arbitrary reference temperature. Another expression of shift factor is (Ferry, 1970)

$$\log a_\epsilon = -\,(B/2.303 f_{o\epsilon}) \,/[f_{o\epsilon}/(\beta_f/\beta_\epsilon)(1-2\mu) + \epsilon] \qquad (20)$$

where B is an empirical constant of order of unity, ϵ is the tensile strain, and $f_{o\epsilon}$ is the fractional free volume at zero strain. β_f and β_ϵ are respectively the coefficient of compressibility of free volume and the total compressibility coefficient of the polymer, and μ is the Poisson's ratio (ratio of changes in width to length of polymer). This expression is valid only for the shear relaxation processes. The compressibility ratio is usually of the order of unity. Therefore, there exists a continuous spectrum of relaxation times, which can be defined as follows (Tobolsky and Murakami, 1959) :

$$E_R(t) = E_s(\tau) \exp\{-t/\tau\} \qquad (21)$$

where $E(\tau)$ is the relaxation modulus at a single relaxation time constant, τ, and t is the real time. Another distribution function that is widely used to define the continuous relaxation times is

$$H(\tau) = \tau E(\tau) \qquad (22)$$

$$E_R(t) = H(\tau)\ \exp\ \{-t/\tau)\ d(\ln\tau)$$

where $H(\tau)$ is usually referred as the relaxation spectrum. Approximation methods have been devised to obtain $H(\tau)$ curves from the experimental $E_R(t)$ curves. The first approximation method is by Alfrey (1948)

$$H_1(\tau) = -(1/2.303)[d(E_R(t))/d(\log t]_{t=\tau}) \qquad (23),$$

while the second method is by Ferry and Williams (1952)

$$H_2(\tau) = H_1(\tau)/\gamma(1+m) \qquad (24),$$

$$m = -\ d(\log H\ (\tau))/d(\log\tau)$$

or by Schwarzl and Staverman (1953)

$$H_2(\tau) = -d(E_R(t))/d(\ln t) + (1/3)d^2E_R(t)/d(\ln t)^2 \qquad (25)$$

where γ represents the gamma function. Ferry (1970) showed plots of H for eight different polymers from viscoelastic liquids (uncross-linked polymers) to solids (Figure 1). The features of the eight polymers are outlined below:

I. A dilute polymer solution whose viscoelasticity is a relatively minor perturbation of the Newtonian behavior of the solvent.

II. An amorphous polymer of low molecular weight to illustrate the effects of short segments of a moving chain.

III. An amorphous polymer of high molecular weight to illustrate the effects of "entanglement", which is the entwining of molecular chains.

IV. An amorphous polymer of high molecular weight with long side groups to illustrate the effect of the degree of entanglement as compared to sample III.

V. An amorphous polymer of high molecular weight below its glass transition temperature to illustrate the difference of effects with samples III and IV.

VI. A lightly cross-linked amorphous polymer to illustrate the effects of long-range rearrangements of chains.

VII. A very lightly cross-linked amorphous polymer to illustrate the effects of cross-linking.

VIII. A highly crystalline polymer which is a composed of a matrix of crystalline material with units of various form such as lamellae and fibrils.

At long periods of time, H should vanish when steady-state flow is achieved. This phenomena is characteristic of the viscoelastic liquids I to IV. For the viscoelastic solids, V to VIII, H attains low values at long times but give no evidence of approaching zero. This behavior is associated with the relaxation of the polymer chains which continues apparently indefinitely.

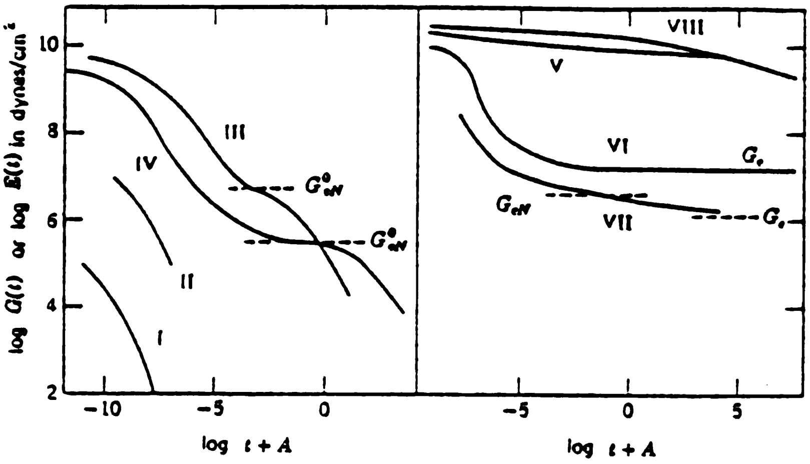

Figure 1. The relaxation spectrum, plotted with logarithmic scales for the eight typical polymer systems. Viscoelastic liquids on left, viscoelastic solids on right, identified by numbers as described in the text. (Ferry, 1970).

V. Water Moisture Effects

Besides temperature and organic vapor effects on phyical and mechanical properties of barrier films, water (i.e. relative humidity) has a tremendous effect on the free volume. This effect has been described extensively in the literature, especially with diffusion and sorption studies in polymers. Water molecules are relatively small. In liquid and solid states, water is strongly associated with itself. In certain polymers, it is associated through hydrogen bond formation.

Long and Thompson (1954) studied the effect of water on three polymers; cellulose acetate, polyvinyl acetate, and polystyrene. They found that the rate of diffusion ofacetone is markedly faster for a mixture of water and organic vapor than for the pure organic vapor for the acetate samples. As for benzene diffusion into polystyrene, the rate was normal. The reason given for the rapid diffusion was that the water acted as a plasticizer in the polymer film itself. As for the non-acceleration sample, polystyrene sorbs only very small amounts of water.

Plasticization is primarily a breaking and reformation of hydrogen bonds in the polymer, that is, a "loosening" of the structure to allow further water migration and permeant penetration. Rogers et. al. (1956) described it as lowering the cohesive energy density and increasing the mobility of the chains.

Barrie et al (1974) in their studies, found that the diffusion coefficient, D, decreases with concentration of water for three polyurethane elastomers, even though that there exists a comparatively strong interaction between the water and the polymer. The results suggested that the water molecules tended to cluster through hydrogen bond formation and that this clustering effect tend to reduce the diffusion rate.

The differences between the results of the studies of Long and Thompson (1954) and Barrie (1974) can be attributed in part to the characteristics of the polymers studied, namely the hydrophilic/hydrophobic nature of the polymer structures. The increase of diffusion coefficient with water vapor concentration is most marked with the polar polymers. A localization of the initially sorbed water over a number of sites increases diffusion (Barrie, 1968). As for the diffusion decreasing with concentration, these polyurethane polymers are usually less hydrophilic and may even be polar. The clustering effect initiates at polar centers or, for the harder plastics, in microcavities existing in the polymer matrix (Barrie, 1968). There is a third option and that is, the diffusion coefficient for water vapor is constant in hydrophobic polymers. The presence of water has little or no effect on the diffusion of the penetrant, water vapor or organic vapor, because the polymers interacts very little with the water molecules.

The effect of water vapor on the oxygen barrier properties of the hydrophilic polymer, ethylene vinyl alcohol copolymer (EVAL) has been the subject of recent studies. Ethylene vinyl alcohol copolymers (EVAL) are excellent oxygen barriers when used under dry conditions. However with increasing relative humidity, oxygen permeability increases. A study by Wachtel et. al. (1984) showed that the permeability gradually decreases at relative humidities below 60%, but increases rapidly at relative humidities above 80% RH. When the polymer is dry there is very little permeation through the amorphous regions because interchain hydrogen bonding reduces the mobility of the polymer chain segments preventing rapid diffusion of oxygen. When moisture is present, it plasticizers the EVAL and reduces the amount of hydrogen bonding. Moisture lowers the glass transition temperature, which is 60 - 70 °C for dry EVAL to below room temperature, thereby changing the physical structure of the polymer from glassy to the rubbery state (Kuraray).

A phenomenon associated with hydrophilic-polar polymers is swelling effects, which is the sorption of permeant (i.e. water or even organic vapor) by the polymer matrix to such an extent that the matrix expands in dimension. The stress developed is then relieved by molecular relaxation processes, such that the chemical potential barrier to the sorption of permeant is reduced leading to further sorption.

Materials

Samples

Ethylene Vinyl Alcohol copolymer (EVAL) film samples were provided by Cryovac Division of W.R. Grace and Company, P.O. Box 464, Duncan, SC 29334. The samples were stored at room temperature in desiccator chambers immediately upon receipt and maintained under these conditions until their use in experimental runs. The average thickness of the films was measured to be approximately 1.0 mil (1/1000 inch) using the Model 549 micrometer from Testing Machine, Inc.

EVAL copolymers have a highly symmetrical molecular structure. The molecules are strongly bonded to each other by inter-and intramolecular hydrogen bonding. EVAL are produced in two modifications (Encyclopedia of Polymer Science and Technology, 1985). The first is an ethylene-vinyl alcohol copolymer with ethylene content of 82-90 mol%. This polymer is not a barrier resin and is used as an adhesive. The second EVAL type has a vinyl alcohol content of 60-75 mol%, and is made by hydrolyzing ethylene-vinyl acetate copolymer (EVAC) with a vinyl acetate content of 78-90 wt%. This polymer type offers superior barrier properties, excellent transparency, high oil and solvent resistance, and good thermal processibility and weatherability (Kuraray).

The EVAL film provided by Cryovac for the studies was of the second type, and exhibited superior barrier properties. Kuraray Company reported two types of EVAL, Types E and F. Type E have good ultimate tensile strength, excellent moisture vapor (90% RH) barrier but fair oxygen barrier. Type F has high tensile strength, superior oxygen barrier but poor moisture vapor (90% RH) barrier. The film supplied by the company was EVAL F.

Toluene

Toluene which meets ACS standards, boiling point of 110.2-110.6°C from Mallinckrodt Inc., Paris, Kentucky 40361 was used as the permeant.

Nitrogen Gas

Dry nitrogen of 99.98% purity was provided by the Union Carbide, Linde Division, Daudery, Connecticut. The N_2 was used as the vapor generator for relative humidify and the permeant vapor.

Water

Deionized water were obtained from a series of conditioners, composed of an Elgin mixed bed deionizer with a resin refill exchange and a Culligan water conditioning with a Ametek activated carbon adsorption filter.

Salt Solutions

The salt solutions used for preparing the required relative humidity were Potassium Acetate (20% RH), Magnesium Nitrate (50% RH), and Ammonium Sulfate (80% RH) at the temperature of 80 °C.

Humidity Sensor

The relative humidity was measured by the Hygrodynamics Hygrometer Humidity Sensors which are capable of temperature measurement as well as relative humidity measurement in a hydrocarbon atmosphere. The sensors are attached to a Hygrometer Indicator whose dial readings are accurate to ±1.5% R.H. over a temperature range of 40 to 120 °F. These Hygrometer Sensors and Indicator were supplied by the Hygrodynamic, Inc., Silver Spring, Maryland.

Permeability Cell

The cell is composed of two 50 cc volume stainless steel or aluminum disk-shaped plates and a hollow central plate for the permeant flow. A Viton O-ring, a fluorocarbon elastomer which is resistant to attack and swelling by most organic vapors, is used as the sealant between the film and the metal. The O-ring creates a hermetic isolation of the chambers from each other and from the atmosphere. As shown in Figure 2, the two cell plates and the center plate are equipped with an inlet and outlet valve and sampling port.

Apparatus

Humidifier System

The humidifier system consists of a nitrogen tank, a gas washing bottle with a fritted dispersion tube and two rotameters. The bottle contained deionized water. Nitrogen gas is flowed through the bottle at a regulated flow rate, thus generating humidified nitrogen vapor. This vapor is mixed with dry nitrogen flow to attain the required relative humidity. The relative humidity is verified by a hygrometer sensor attached at the outlet flow. To reduce condensation, temperature of the flow is

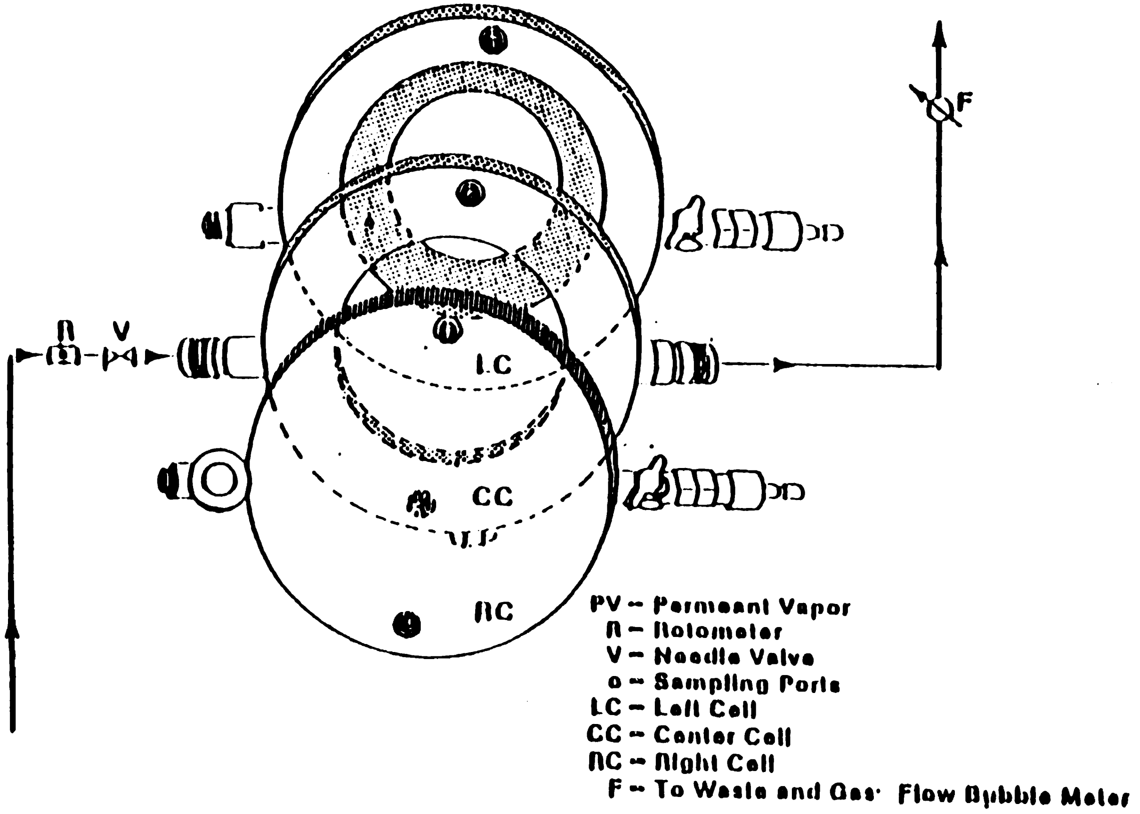

Figure 3. Schematic diagram of Preconditioning System and Permeation System

maintained at least 2 °C above ambient temperature by a water bath tank. As illustrated in Figure 3, the preconditioning system can accomodate 3 cells at each relative humidity.

Permeation System

The permeation test system is composed of three gas washing bottles with fritted dispersion tubes, a water bath tank and five rotameters. Nitrogen gas is flowed at a low flow rate into a gas washing bottle (B1) containing a mixture of toluene and deionized water, thereby generating a saturated humidified permeant stream. This vapor can be adjusted to the desired humidity or concentration by regulating the flow of dry nitrogen (nitrogen tank) or humidified nitrogen (from gas washing bottle B2) or dry toluene (from gas washing bottle B3) to the humidified permeant flow stream. The humidity of the permeant is measured at the outlet using the hygrometer sensor attached to a Hygrometer Indicator. The temperature of the system is maintained at least 2 °C above ambient temperature by a water bath tank. As illustrated in Figure 3, the apparatus is capable of performing multiple runs concurrently. A combination of four cells can be attached to a dispensing manifold respectively. Gas flows were regulated with NU PRO needle valves, type B-2SG.

SCHEMATIC OF PERMEATION TEST APPARATUS
FOR EVALUATING THE EFFECT OF RELATIVE HUMIDITY
ON THE PERMEATION OF ORGANIC VAPOR

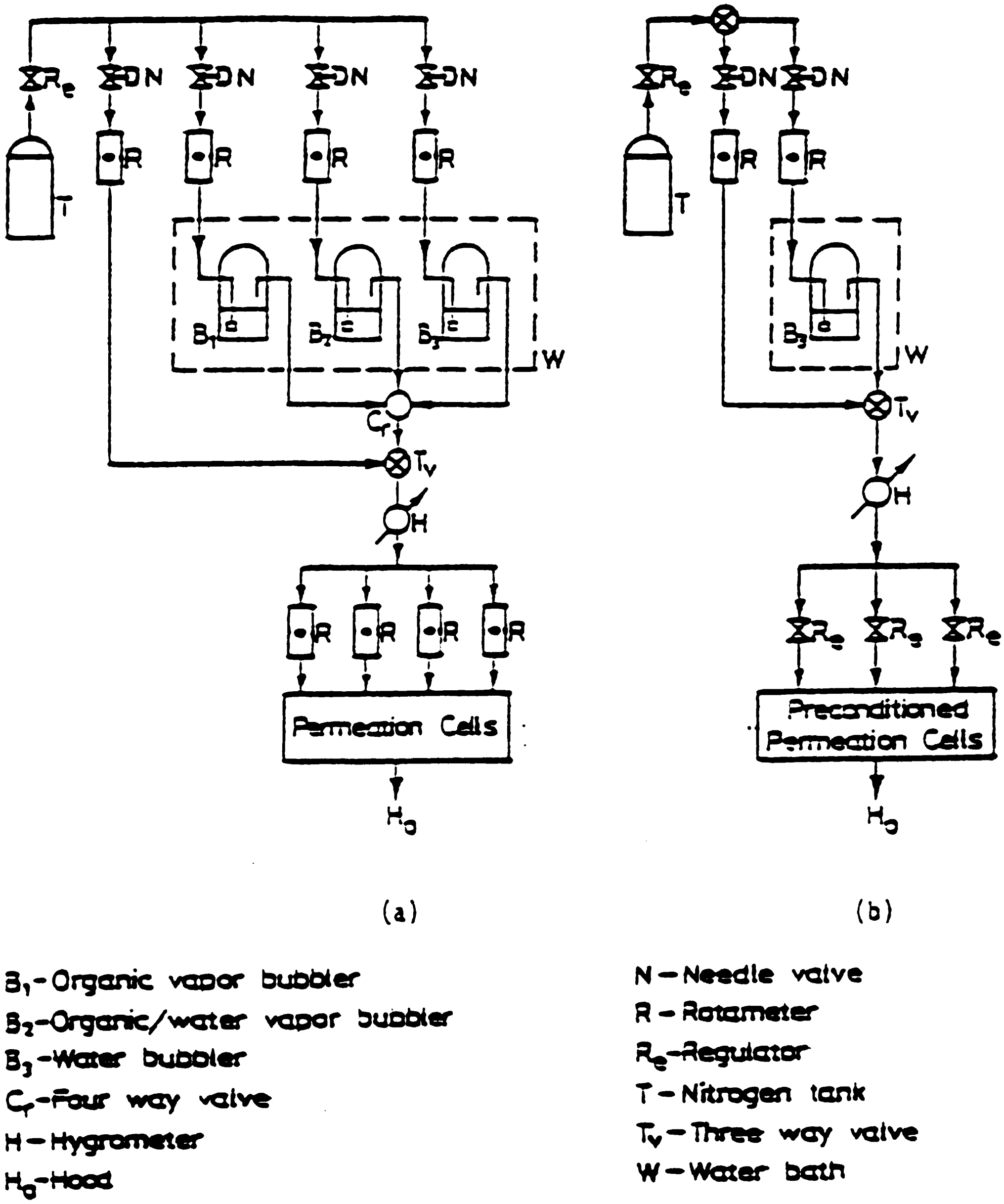

Figure 2. Schematic diagram of Permeation Cell

Gas Chromatograph

The gas chromatograph used for detecting the permeant concentration is the Model 5830 Hewlett Packard with dual-flame ionization detection. The detector is linked to a 18850 GC Hewlett Packard integrator. The conditions of the gas chromatograph are listed in Table 1. Known quantities of toluene were dissolved in liquid o-dichlorobenzene to create standards for the calibration of the gas chromatograph.

Table 1. Gas Chromatograph Conditions

Temperature	150 °C
Injection temperature	175 °C
FID temperature	350 °C
Oven maximum temperature	225 °C
Carrier flow (Helium)	40 psi
Time 1	10 min

The average for several determinations gave a factor of 5.27 x 10^{11} units per gram of toluene. Since the partial pressure of toluene when mixed with nitrogen in the permeation experiments was in the order of 1 x 10^{-2}

atm, applying an ideal gas behavior, the above factor was equivalent to 3.4 x 10^{-6} g/cc (3.4 ppm) for each 10^{6} units area in the output of the gas chromatograph.

Tensile Tester

The Tensile Tester used for the stress-strain experiments is the Model TT-C Instron tensile tester. The extensional mode was set at 1 in/min and the relaxational mode at 0.5 in/min. X-head speeds of 0.05, 0.1 and 0.5 in/min were studied for each film sample.

Differential Scanning Calorimeter (DSC)

A DuPont Thermal Analyzer Model 990A was used to measure the thermal transition temperature, Tg, and the melting point of EVAL films. The equipment was supplied by the Michigan Molecular Institute (MMI).

Thermal Mechanical Analyzer (TMA)

A DuPont Thermal Mechanical Analyzer Model 990A was used to measure the specific volume and temperature. The equipment was supplied by the Michigan Molecular Institute.

Procedure

Permeation and Tensile Tests Operations

The films to be tested were removed from the desiccator chamber and cut to a standard of 17x11 cm to conform to the shape of the permeability cell. On each side of the central plate, a film sample to be tested was placed. The cell was assembled tightly and mounted onto the humidifier apparatus for equilibrium preconditioning to a specified relative humidity.

At the outlet of the system, a low flow rate of the specified humidified nitrogen vapor was swept into the central and lower chambers, thereby equilibrating the cell with the required relative humidity. The films were preconditioned for a period of 7 to 10 days. Preliminary tests showed that the films had equilibrated within this period of time with the surrounding relative humidity.

After preconditioning the films, the cells were mounted onto the permeation test apparatus. To maintain a constant specified humidity in the left and right sides of the central chamber, the specified humidity for the run was swept through the chambers before the sample ports were closed.

A constant low partial pressure of humidified permeant vapor (i.e. less than 100 ppm, wt/v) was flowed continually through the central chamber. This allowed the permeability of two film specimens to be determined concurrently under identical conditions. Unless otherwise stated, permeability runs were carried out at 23 °C and in duplicate. Studies were carried out at three relative humidity conditions, namely 0, 50, 75 and 87.5 %RH, and at several vapor concentrations.

At predetermined time intervals,an aliquot (0.5 ml) of headspace gas was removed from the sample chambers(right or left sides) with a Hamilton gas tight 1750 side-pore syringe and was injected directly into the gas chromatograph. To maintain a constant total pressure in the isolated chambers, the volume of headspace gas removed for analysis was replaced with an equal volume of humidified nitrogen gas (0.5 ml) from the preconditioning system. A constant total pressure of 1 atm was maintained throughout the run in both the central and the isolated chambers.

Measurements were continued until sufficient data was collected to ensure steady state kinetics and that the lower concentration (left and right sides) sample cell chambers did not exceed 3% of the permeant vapor concentration in the central chamber. This was to assure a constant driving force of the penetrant throughout the course of the run. The data collected were analyzed and plotted on a permeation-time plot.

After the run has achieved the steady-state kinetics, the cell is disassembled and the film samples are removed for testing on the Instron tensile tester. Using a commercial sample cutter, the films are cut exactly into three 1- inch width samples. The film is then mounted into the vice grip of the Instron tester separated two inches in length. The stress load on the film is 1 lb. When the load is reached, the extensional mode is switched off and the load relaxation with time is measured on the chart. The film is stretched to about 2 to 3% for all cases. The data obtained were analyzed and plotted on a stress-time plot.

DSC and TMA operations

Film samples were preconditioned to about 20, 50, and 80 %RH using prepared saturated salt solutions following the ASTM E104-51 standard. The samples along with the salt solutions were placed in hermetically sealed containers. Relative humidity measurements were performed each day to ensure equilibrium condition exist in the containers. The samples were preconditioned for approximately 12 days. Dry samples were cut and placed in a glass desiccator. All the samples were brought to MMI for testing, where Differential Scanning Calorimeter analysis were performed.

Samples were weighed and placed in a hermetically sealed capsule. The sealed capsule ensured that the water vapor of the humidified film would not escape to the atmosphere during the heating process. The rate of heating was 10 °C per minute. The temperature range tested was from -20 °C to 125 °C. Nitrogen gas was flowed through the heating chamber at a rate of 20 cc/min. Temperature and heat flow measurements were conducted continually and the information was stored in the DuPont 990A computer. Two samples of the same relative humidity but of differing weights were tested in each run. After each run, the DSC heating element was cooled with liquid nitrogen. The data obtained was plotted as heat flow versus temperature and was analyzed for the Tg at each relative humidity.

Sample size of .25 square inch were used for the Thermal Mechanical Analyzer. The sample was placed in the heating chamber and was heated from -10 °C to 100 °C. The rate of heating was 0.5 °C/min. Nitrogen gas was flowed through the heating chamber at a rate of 20 cc/min. Liquid nitrogen was used as the coolant. A linear expansion probe was used to measure the expansion of the film. Temperature and linear expansion measurements of the film were obtained continually and was stored in the DuPont 990A computer. The data was plotted linear expansion versus temperature and was analyzed for the expansion coefficient.

Water sorption operations

EVAL film samples of known weight were placed in hermetically sealed buckets at known relative humidities, which were obtained using the same ASTM standard as the DSC and TMA operations. Weight measurements were conducted daily until equilibrium sorption for each sample was achieved. The data obtained from the calculated weight differences were plotted as equilibrium moisture content versus relative humidity.

RESULTS and DISCUSSION

Permeation

The results of the effect of relative humidity on the permeability and diffusion of toluene vapor through the EVAL test film are tabulated in Table 2 and presented graphically in Figures 4 and 5, where the permeability constant and diffusion coefficient are plotted as a function of vapor concentration for constant values of relative humidity respectively. Samples 1 and 2 were the only samples studied with a single film cell; all other permeability studies were conducted with a dual-film cell, as described in the materials section. Figure 6 shows a representative of the permeation of toluene vapor through an EVAL test film.

As shown in Table 2, at 0 and 50 %RH, toluene vapor did not permeate through the EVAL film, even after 30 days of continuous testing at a penetrant driving force concentration of 94 - 100 ppm (wt/v). However, at 75 %RH, permeation was observed after 3 days of testing at a penetrant concentration level above 90 ppm (wt/v). Based

Table 2. Effects of Relative Humidity and Vapor Concentration on the Diffusion and Permeability of Toluene Through EVAL Test Film

Samp. No.	%RH	Toluene Conc. (ppm) (wt/v) (±2) (a)	$\overline{P}$ Permeability Constant (g/m day-ppm) (x 10^{-5})		θ Lag Time (min)	D Diffusion Coefficient (sq. in/min) (x 10^{-11})
1.	87.5	87	3.9	(b)	1566	8.6
2.	87.5	91	5.2	(b)	1462	9.2
3.	87.5	99	7.7	(e)	1490	8.6
4	75.0	95	4.0	(e)	5192	2.6
5.	75.0	90	2.8	(e)	3375	4.0
6.	50.0	99	---------(c)	(e)	----	-----------
7.	50.0	94	---------(c)	(e)	----	-----------
8.	0.0	96	---------(d)	(e)	----	-----------

(a) Average concentration measured
(b) Measured with a single film cell attachment
(c) No permeation detected after 30 days or more
(d) No permeation detected after 14 days
(e) Average of replicate runs

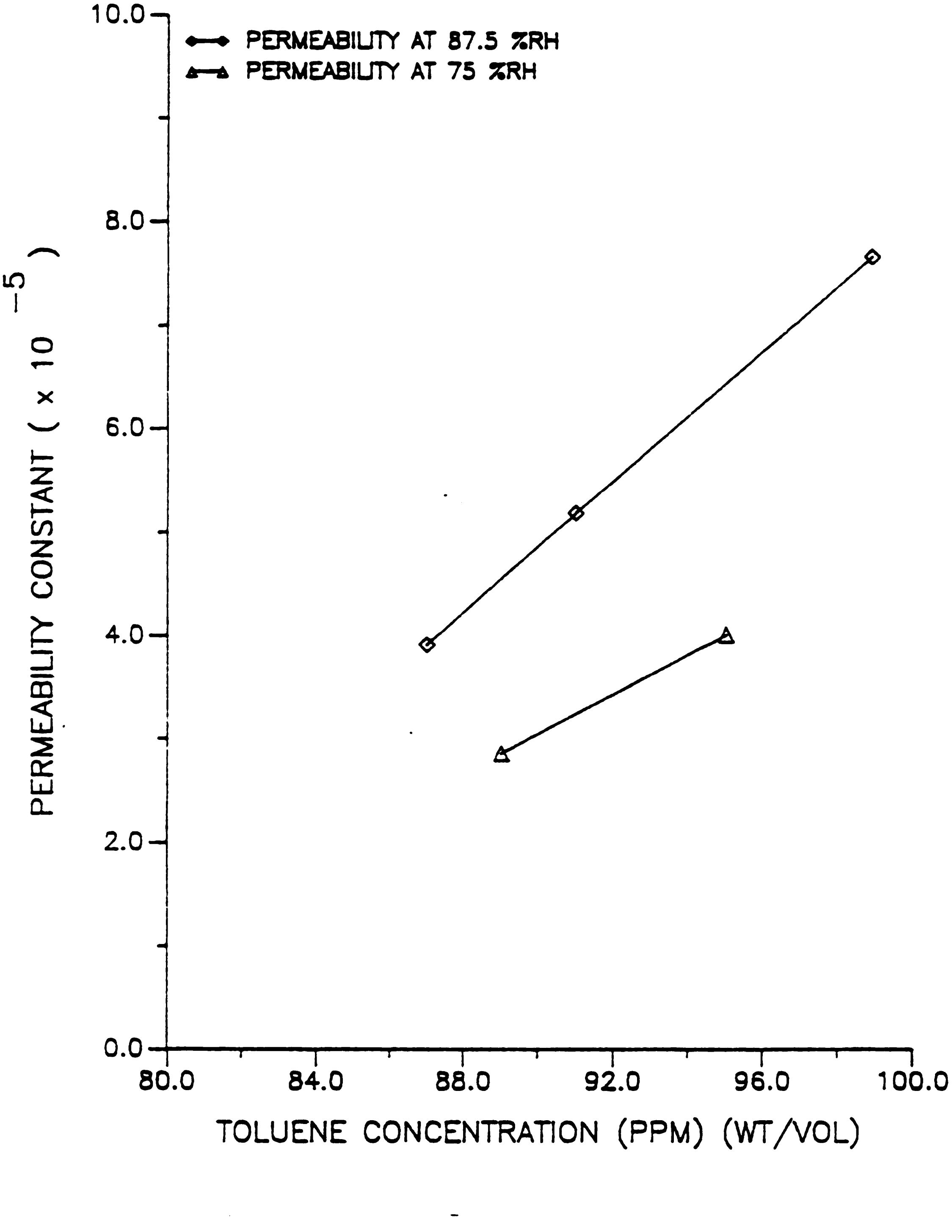

Figure 4. Effects of Relative Humidity and Toluene Vapor Concentration on Permeability Constant

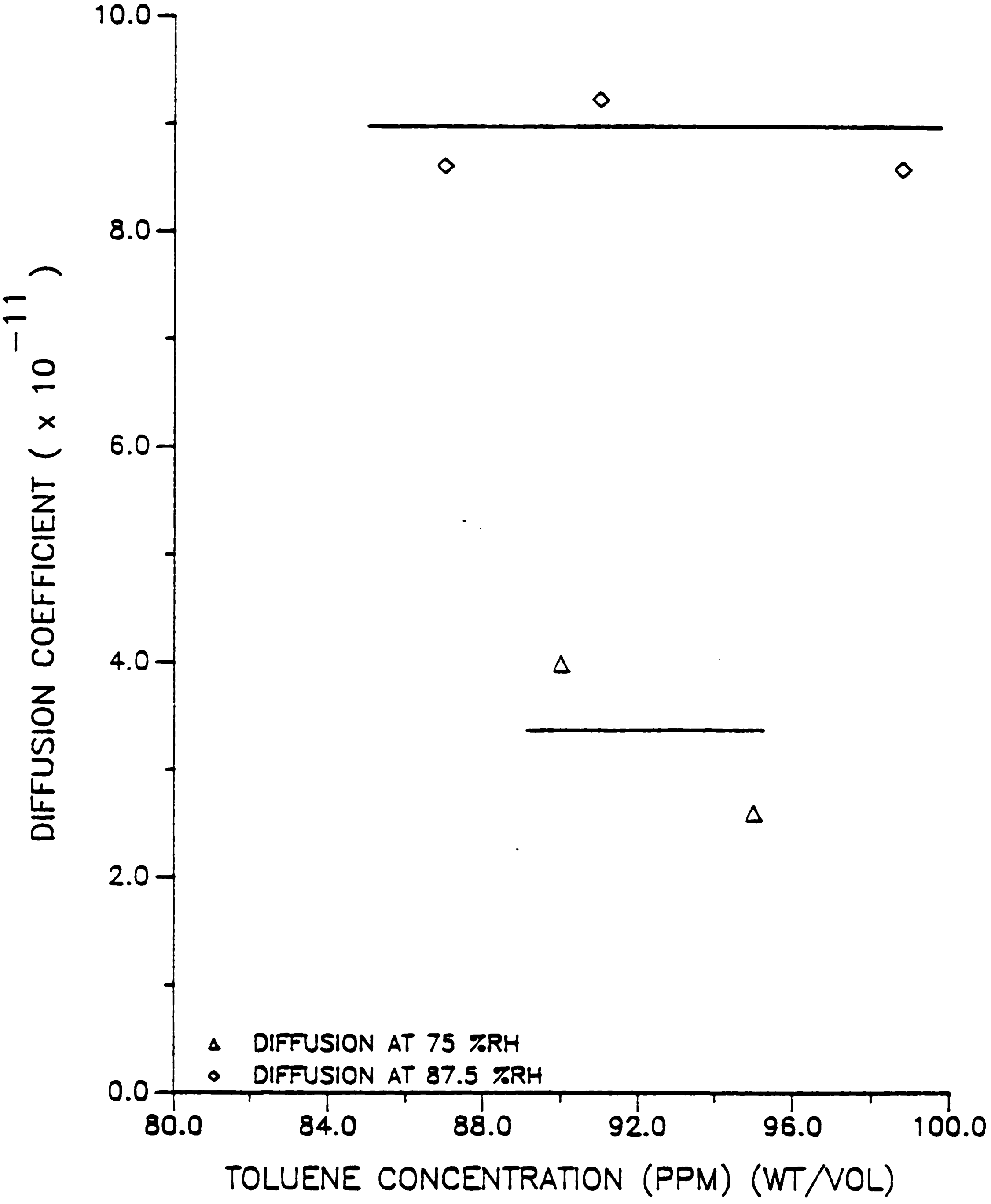

Figure 5. **Effects of Relative Humidity and Toluene Vapor Concentration on Diffusion Coefficient**

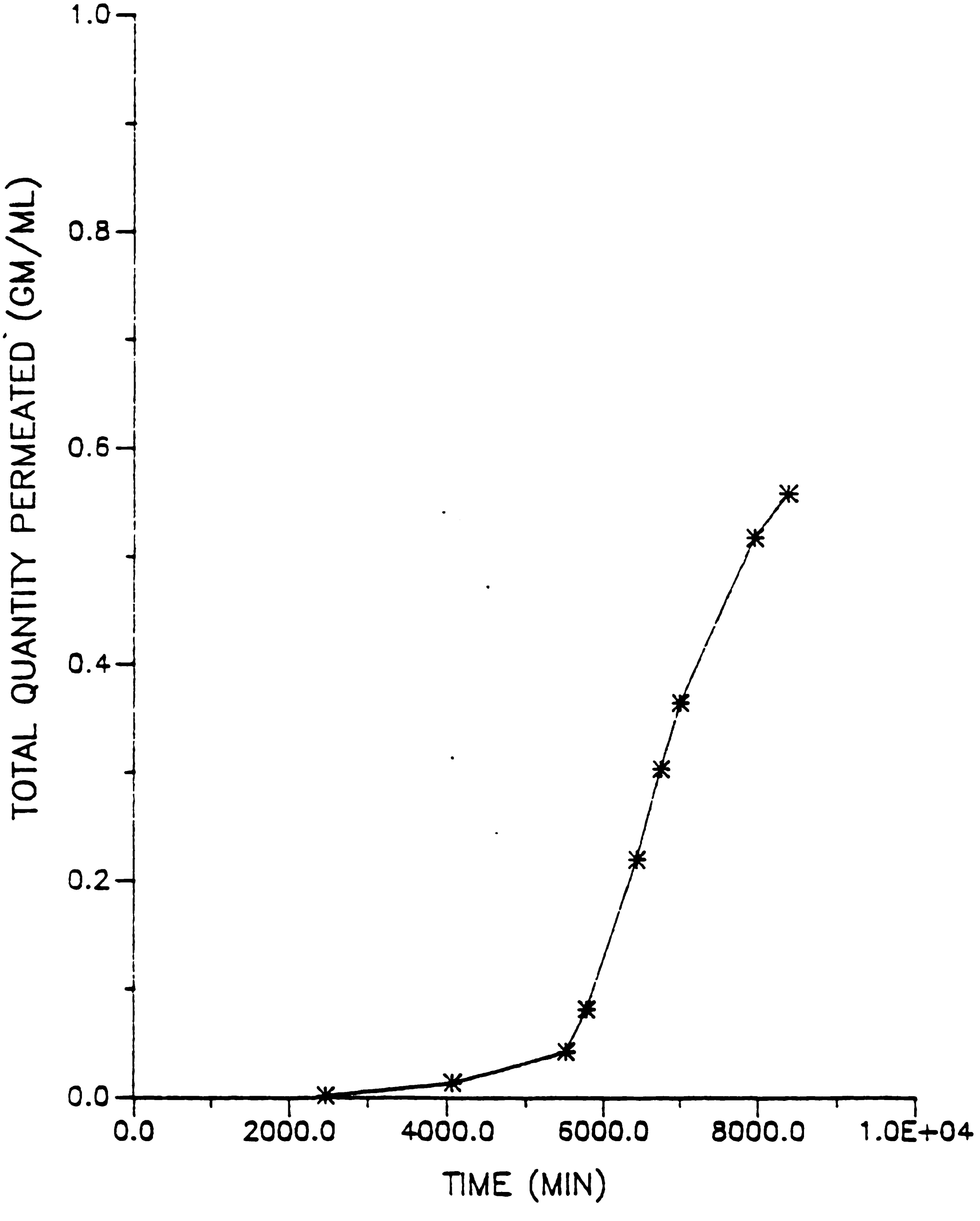

Figure 6. A representative plot of the Transmission Rate of Toluene Vapor through EVAL

on these two results, it was concluded that there exists a threshold relative humidity (i.e. moisture sorbed) above which permeation through the film as well as a penetrant concentration level threshold would proceed at a measurable rate. The results obtained show the importance of relative humidity on the diffusion of organic vapor through the EVAL test film. The relative humidity threshold level was observed between the range of 50 to 75 %RH. This conclusion is similar to other studies using oxygen as the permeant. Wachtel et. al. (1984) found that oxygen permeation increase exponentially above a range of 70 to 80 %RH and that below 50 %RH, oxygen permeation was quite low.

From Figure 4, the permeability data obtained at relative humidities of 75 and 87.5 %RH respectively, showed an increasing linear relationship with permeant concentration. Also shown in Figure 4 is the strong dependence of permeability on relative humidity at constant vapor concentration. These findings are presented graphically in Figure 7 wehere a plot of permeability versus percent relative humidity is shown and in Figure 8 where the permeability constant is plotted as a function of the equilibrium moisture content sorbed. As shown by both Figures 7 and 8, permeability increases with increasing relative humidity at a constant vapor concentration.

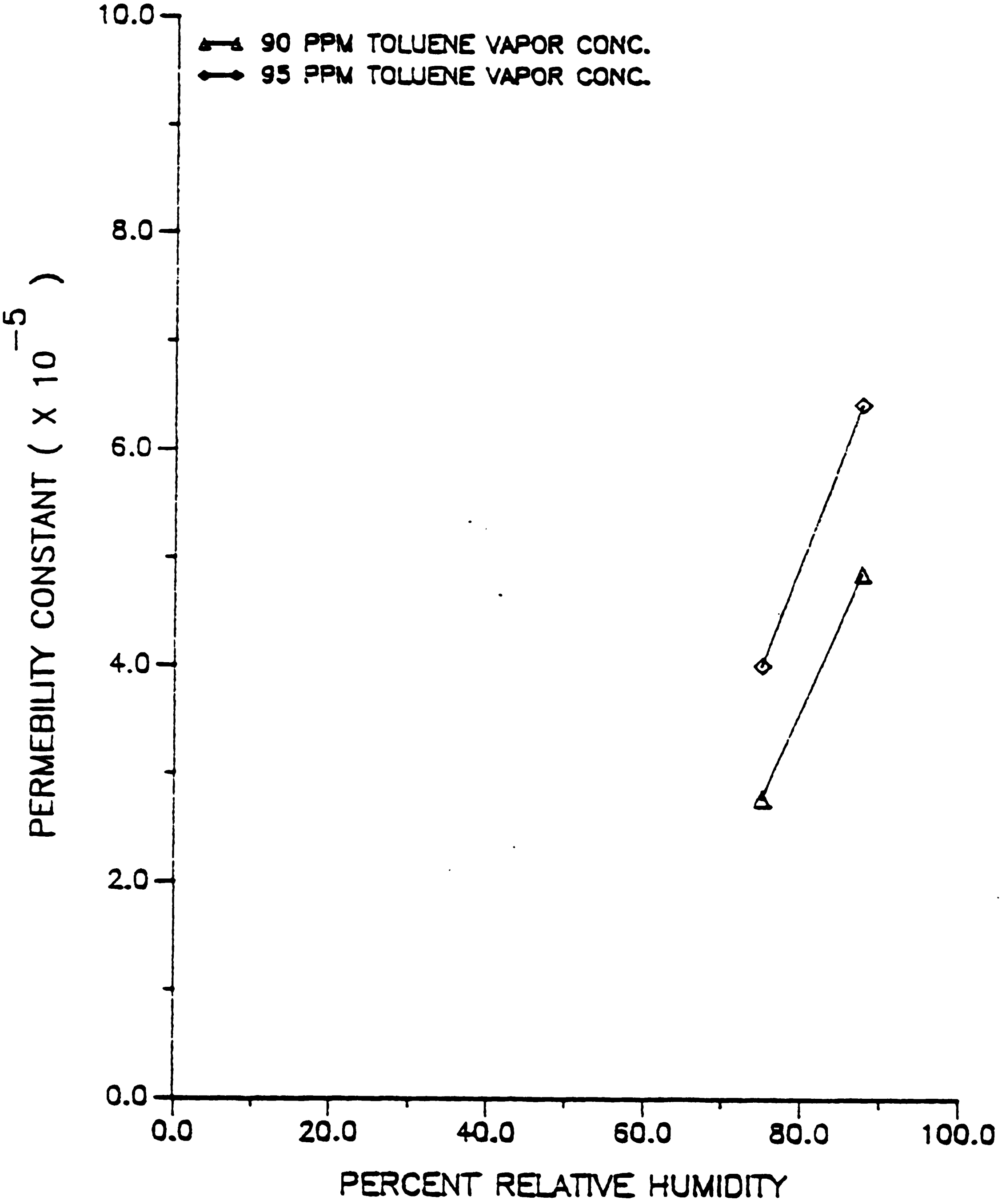

Figure 7. Effects of Relative Humidity on Permeability Constant at specified Toluene Vapor Concentration

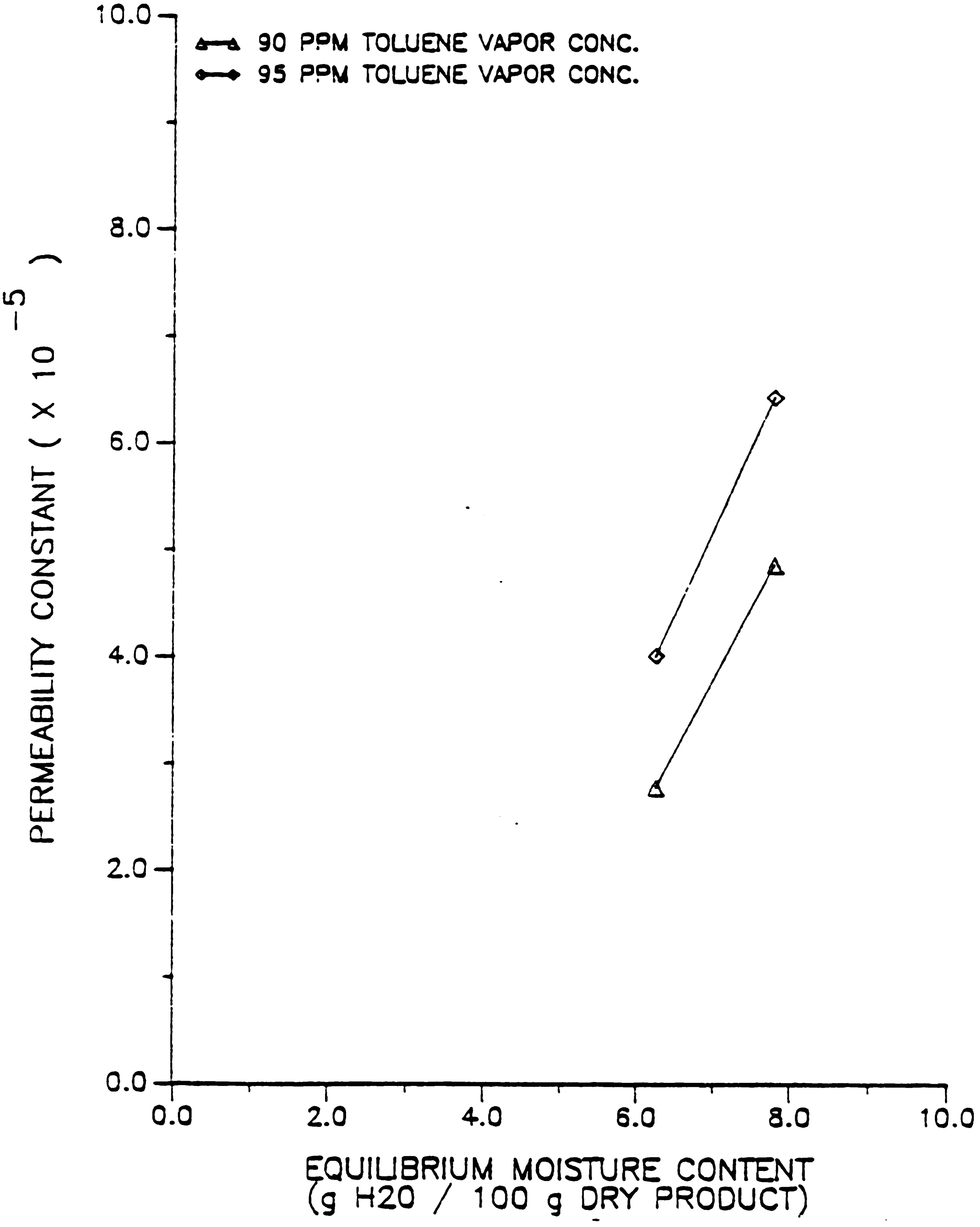

Figure 8. Effects of Equilibrium Moisture Content on Permeability Constant at specified Toluene Vapor Concentration

From Figure 5, the diffusion coefficient data showed a relative humidity dependence and an concentration independence. Increasing the relative humidity at a fixed vapor concentration increases the diffusion coefficient.

A possible mechanism to explain the water vapor effect on toluene vapor permeating through laminated EVAL was proposed by Liu (1986). The sorption of water vapor into a polymer matrix acts as a plasticizer and causes an increase in segmental motion of the polymer chain. As the amount of water sorbed increases, the polymer chain segmental mobility increases, thereby leading to an increase in toluene vapor diffusivity. It was also proposed that the laminated EVAL films were in a glassy state (i.e. above Tg) when dry but became non-glassy as water vapor is sorbed into the polymer matrix (i.e. below Tg). When dry, the interchain hydrogen bonding of the polymer matrix reduces the mobility of the polymer chain segments present. When moisture is present, it reduces the amount of hydrogen bonding. The effect of equilibrium moisture content on the glass transition temperature of the EVAL film studied provided supportive evidence for this proposed mechanism. These studies are described in detail in a later section (i.e. Glass Transition Temperature).

Water Sorption

The result of the equilibrium sorption of water by EVAL samples is listed in Table 3 and is plotted in Figure 9 as the equilibrium moisture content versus relative humidity.

Table 3. Equilibrium Moisture Content of EVAL at Varying Relative Humidity

Relative Humidity	Equilibrium Moisture Content (g H20 / 100 g Dry Product) ($\pm$0.02)	
	Experiment(a)	Literature(c)
0	0.0(b)	0.0
20	1.6	0.9
50	3.71	2.4
85	7.48	6.1

(a) Average of three replicates at 80 °F.
(b) Assumed zero moisture content
(c) Kuraray Co., Ltd. literature

The experiment data was best fitted with a quadratic equation and is given as:

$$emc = A + B*(RH) + C*(RH)^2 \qquad (26)$$

where emc is the equilibrium moisture content in units of g H20 / 100 g Dry Product, RH is the relative humidity, A = 0.772, B = 3.0×10^{-2}, and C = 5.743×10^{-4}, and the literature data is given as:

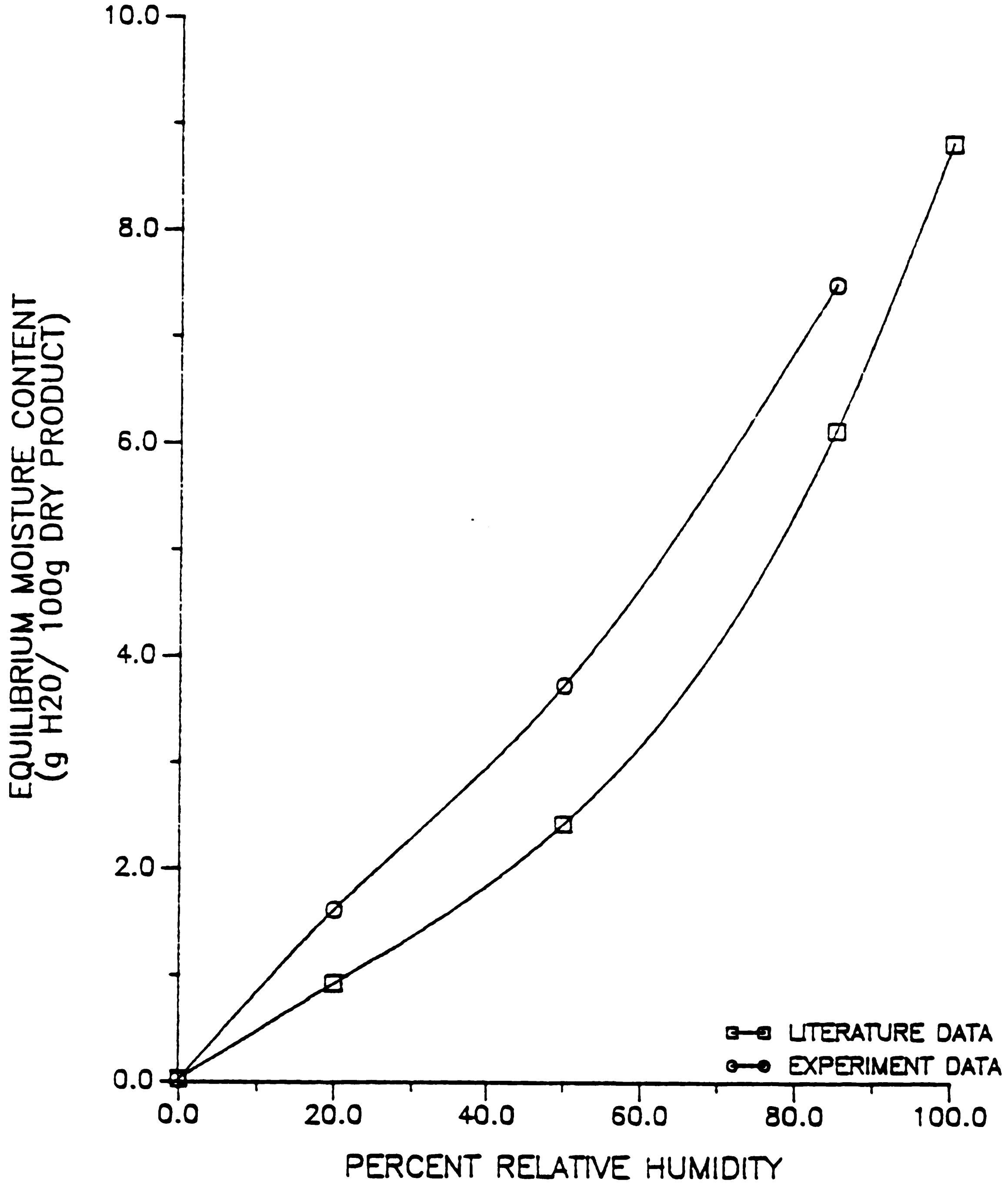

Figure 9. Plot of Equilibrium Moisture Content versus Relative Humidity

$$lemc = D + E*(RH) + F*(RH)^2 + G*(RH)^3 \qquad (27)$$

where lemc has the same units as emc, $D = 3.066\text{x}10^{-3}$, $E = 5.019\text{x}10^{-4}$, $F = -4.623\text{x}10^{-4}$, and $G = 8.42\text{x}10^{-6}$.

Experiments were conducted to determine the initial moisture content of dry EVAL samples held in the desiccators. The results showed that the initial moisture content of dry EVAL samples was essentially zero moisture content (i.e. at a level below the detectability of the gravimetric equipment).

The results of the gravimetric sorption experiments (Figure 9) showed an increasing equilibrium moisture content with increasing relative humidity. Kuraray Co.,Ltd. reported a similar trend in their analysis of EVAL F. Comparison between Kuraray reported values for EVAL F and the gravimetric results showed only a 1% difference (see Figure 9). This difference can be accounted for by different resins sources being used by Cryovac and Kuraray, as the percent ethylene present in the film may vary.

Glass transition temperature

The transition from glass to rubber states is effected over a range of temperatures, as seen in Figures 10A to 10H. The lower and upper bounds of this range maybe identified as points on the slope of the heat flow with temperature curve. The first discontinuity of the slope on the curve, as the temperature is increasing, is the lower bound and is defined as Tg(lower). The second discontinuity of the slope is the upper bound and is defined as Tg(upper). Comparing the DSC figures, the difference between Tg(upper) and Tg(lower) are observed to decrease as the relative humidity is increased (i.e. water sorbed). A proposed mechanism to explain this phenomena is that at 0 %RH, the EVAL film is a semi-crystalline polymer of fixed fraction of crystalline and amorphous matrix. As the water sorbed is increased, the crystalline fraction is decreased by the plasticization effects of water. Hence, the EVAL at a high relative humidity would have a less crystalline fraction than at 0 percent relative humidity and would show a small range of Tg, as observed in Figures 9G and 9H at the 80 %RH.

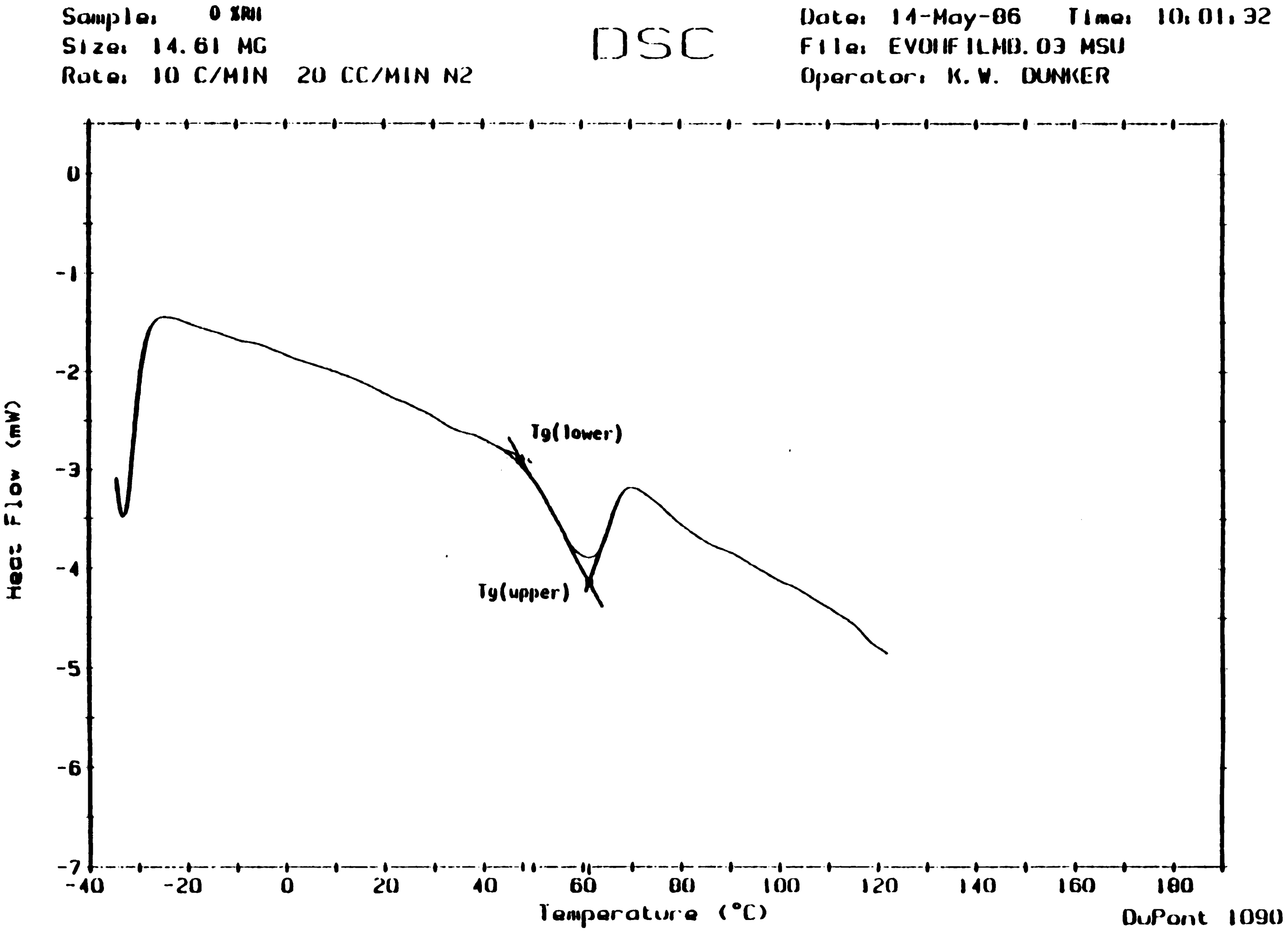

Figure 10A. Plot of Differential Scanning Calorimeter Analysis of Glass Transition Temperature at 0 Percent Relative Humidity

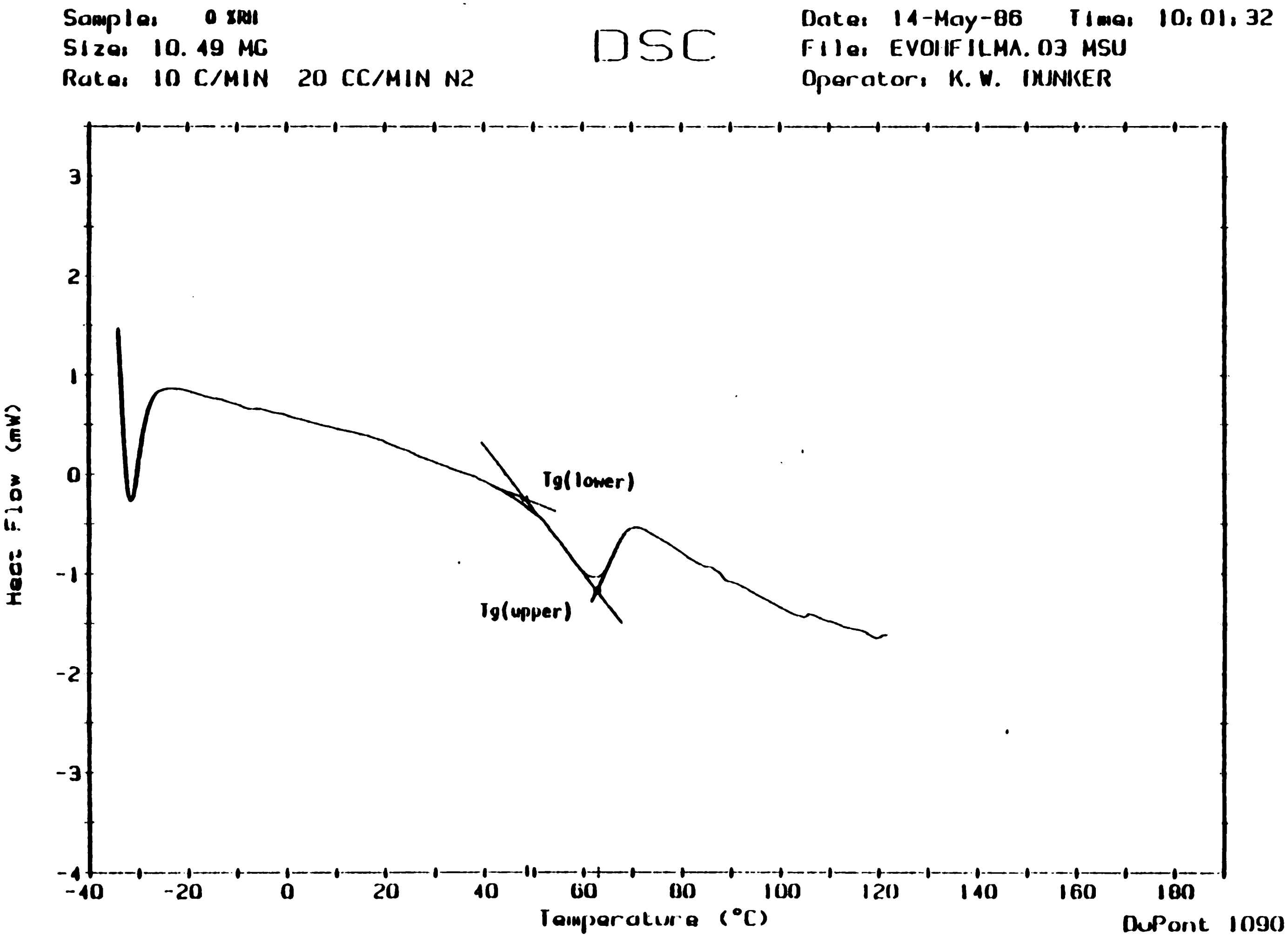

Figure 10B. Plot of Differential Scanning Calorimeter Analysis of Glass Transition Temperature at 0 Percent Relative Humidity

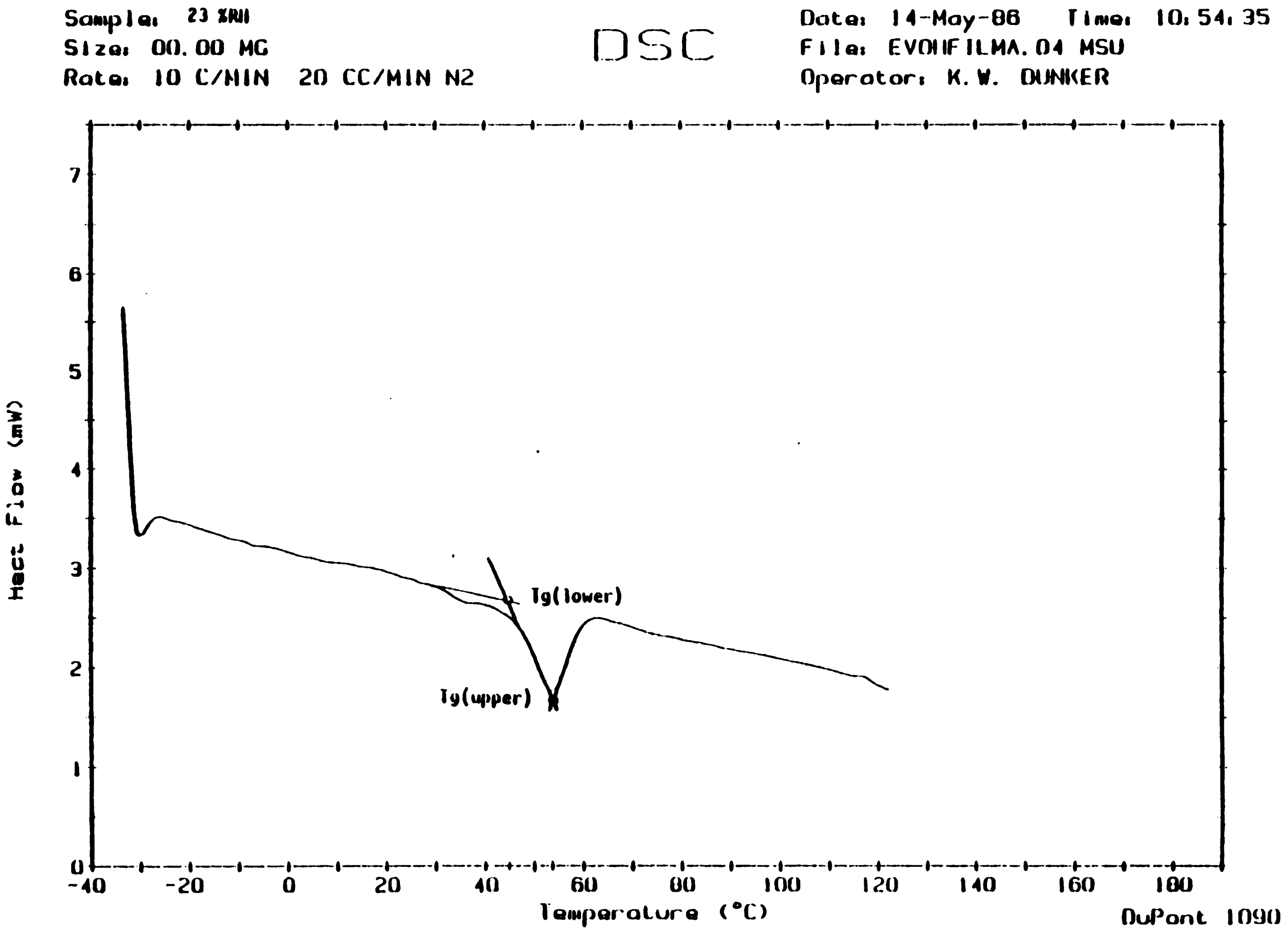

Figure 10C. Plot of Differential Scanning Calorimeter Analysis of Glass Transition Temperature at 23 Percent Relative Humidity

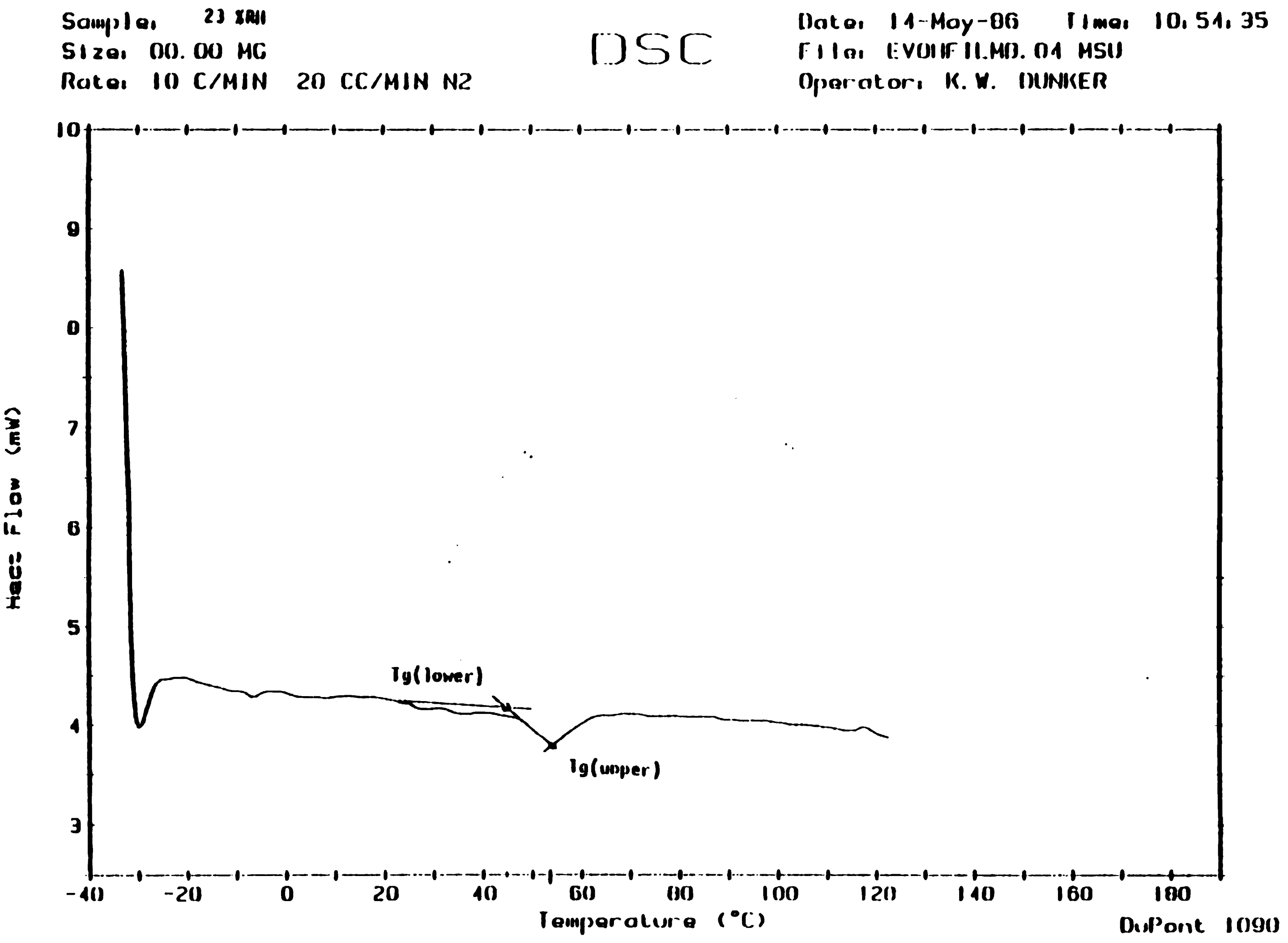

Figure 10D. Plot of Differential Scanning Calorimeter Analysis of Glass Transition Temperature at 23 Percent Relative Humidity

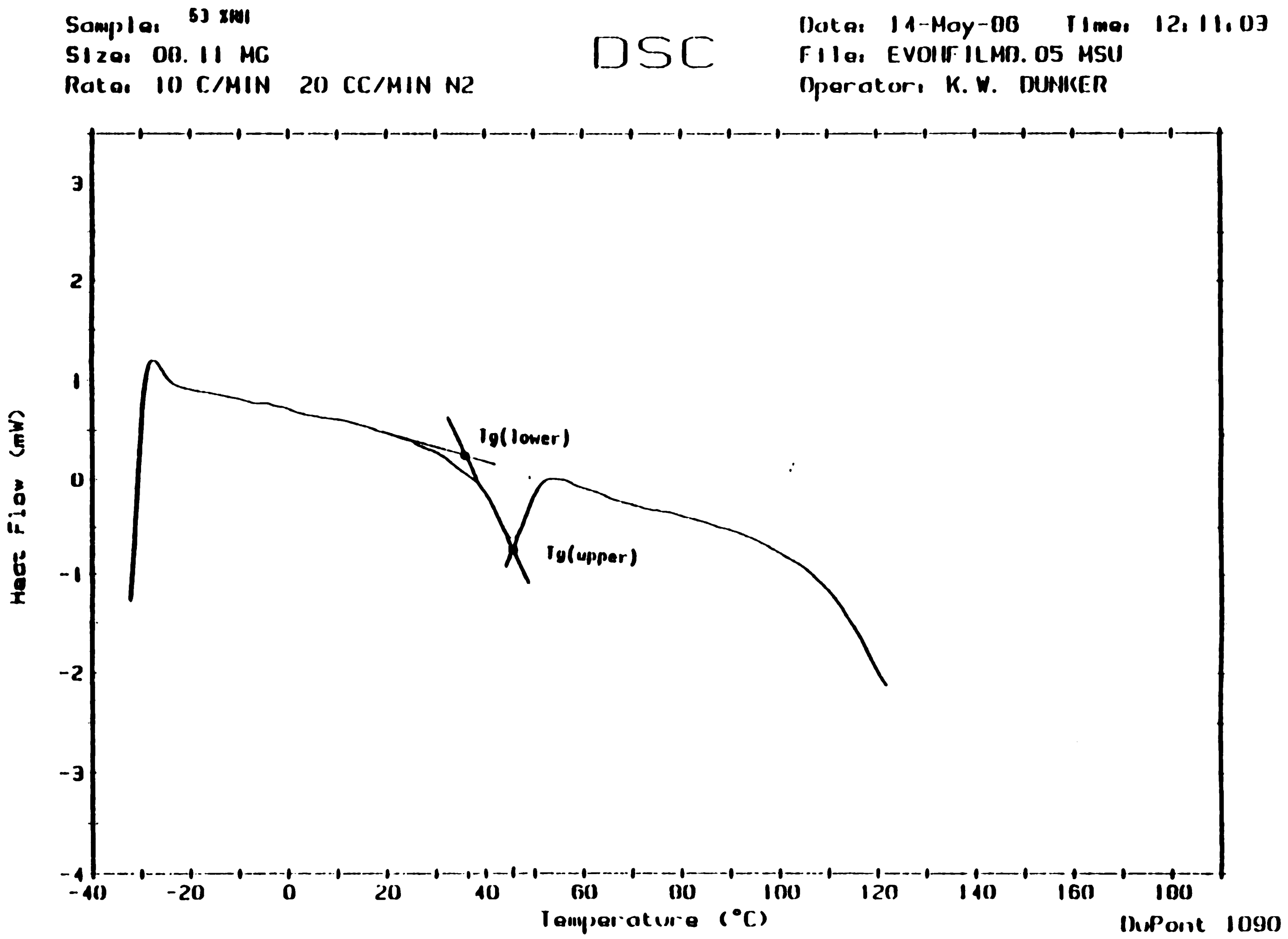

Figure 10E. Plot of Differential Scanning Calorimeter Analysis of Glass Transition Temperature at 53 Percent Relative Humidity

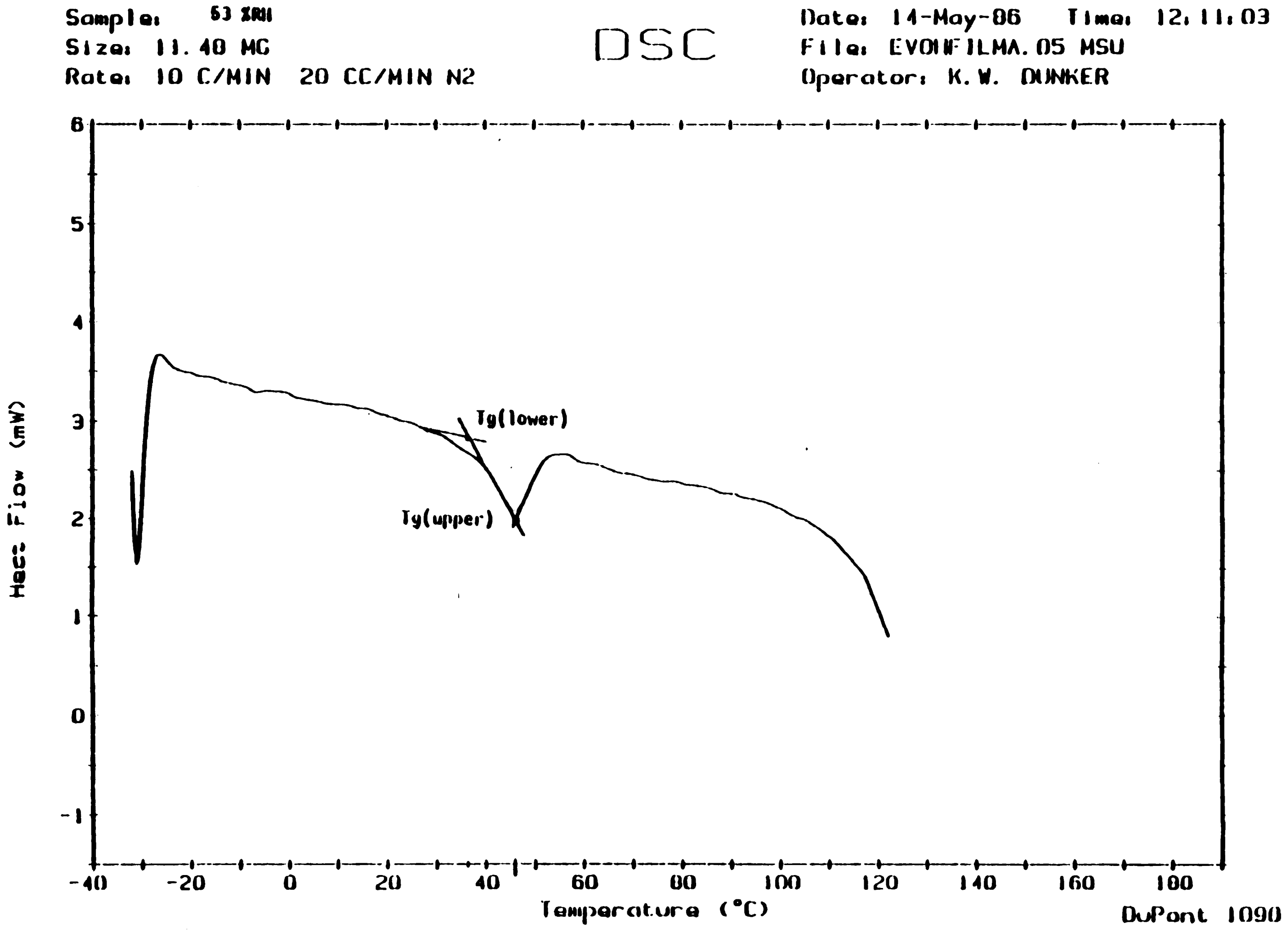

Figure 10F. Plot of Differential Scanning Calorimeter Analysis of Glass Transition Temperature at 53 Percent Relative Humidity

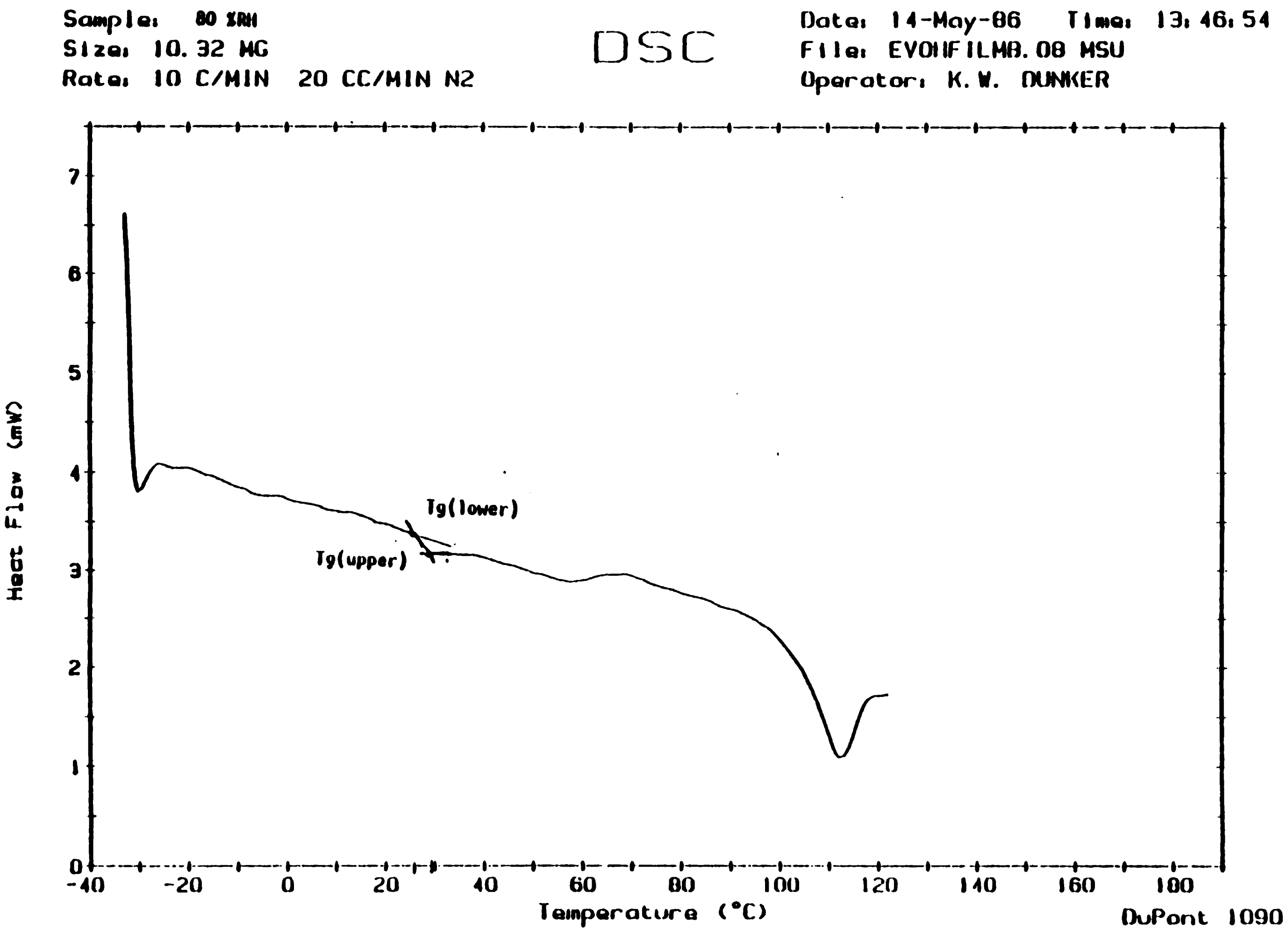

Figure 10H. Plot of Differential Scanning Calorimeter Analysis of Glass Transition Temperature at 80 Percent Relative Humidity

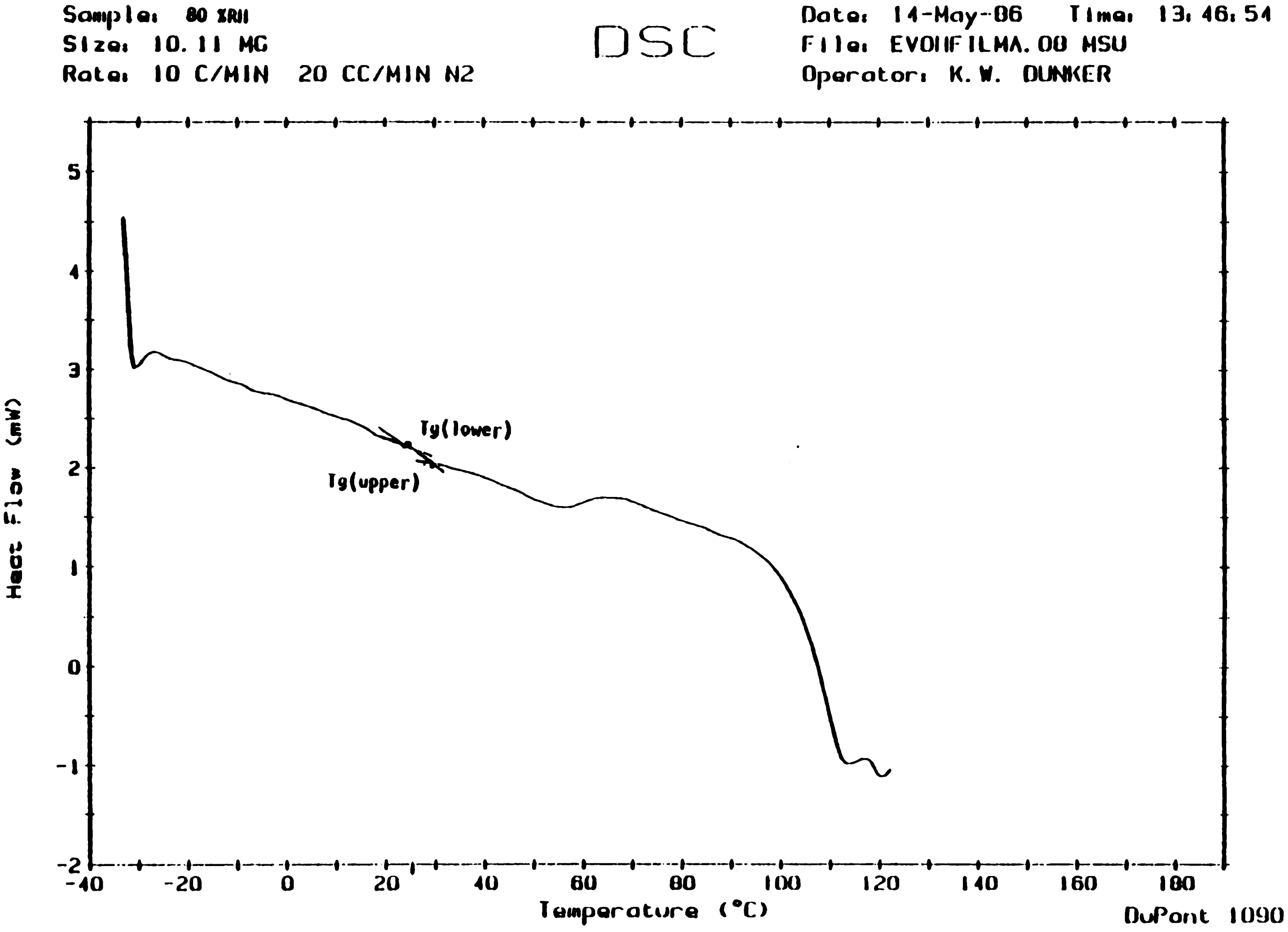

Figure 10G. Plot of Differential Scanning Calorimeter Analysis of Glass Transition Temperature at 80 Percent Relative Humidity

The Tg(lower) and Tg(upper) are tabulated in Table 4 and is presented graphically as the temperatures versus percent relative humidity or equilibrium moisture content (see Figures 11 and 12 respectively).

Table 4. Effects of Relative Humidity on Glass Transition Temperature of EVAL

%RH	Equilibrium Moisture Content (g H2O/100 g DRY PRODUCT)	Glass Transition Temperature (± 2 °C)	
		Tg(lower)	Tg(upper)
0	0.0 (a)	48	61
23	1.77	45	54
53	3.98	36	47
80	6.65	26	30

(a) Assumed zero moisture content

The results of Table 4 were best fitted with a regression equation of the form:

$$\text{Tg(lower)} = A + B*(RH) \qquad (28)$$

$$\text{Tg(upper)} = C + D*(RH)$$

where A = 49.658, B = -0.27969, C = 62.6028, D = -0.37635, and the correlation fit was 0.98. At 50, 75 and 85 %RH, the Tg are 36, 28 and 26 °C respectively with a deviation of 2 degrees. The permeation tests were conducted at room temperature which vary from 22 to 27 °C, but the toluene and water vapor, as described in the materials section,

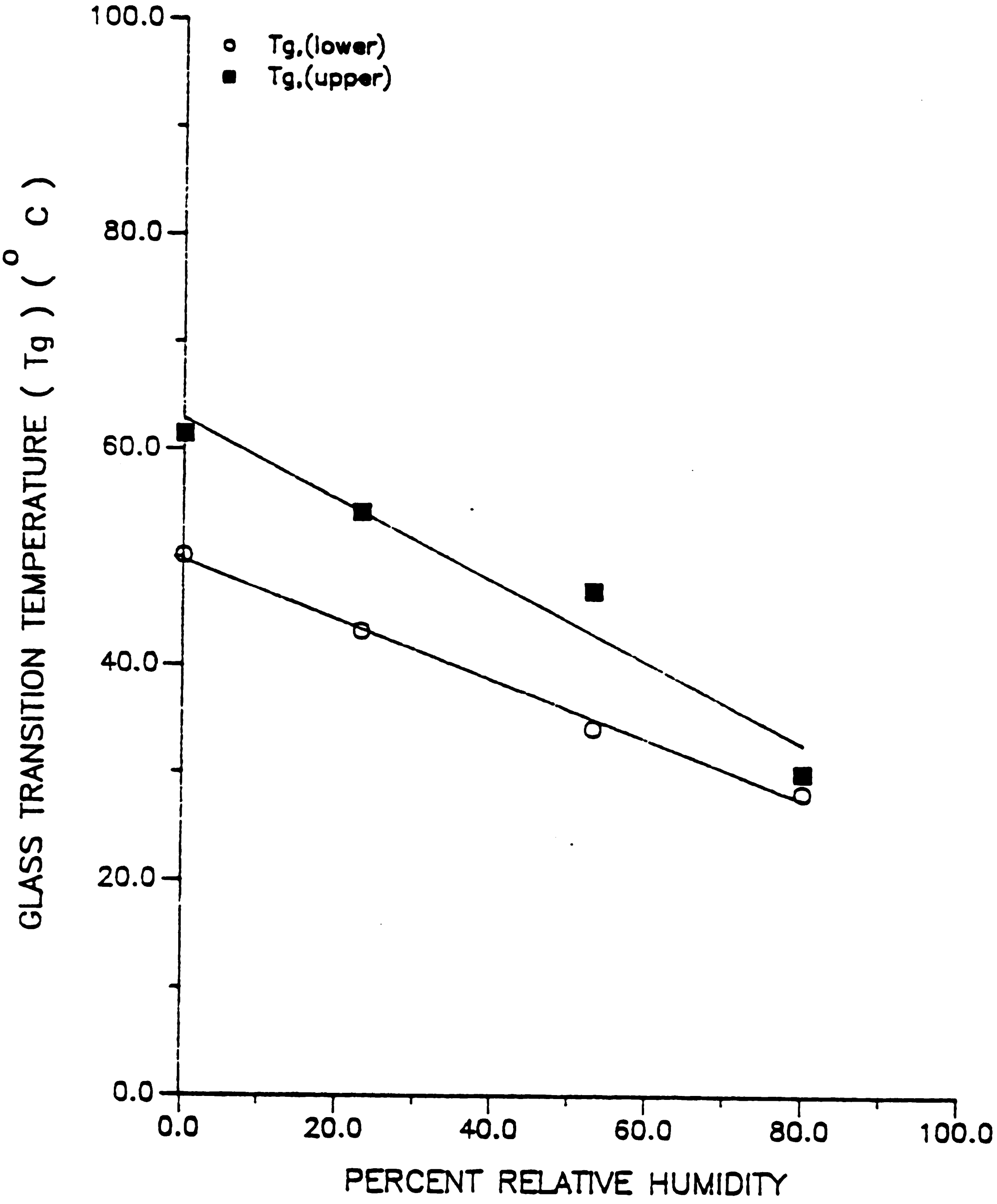

Figure 11. Plot of Glass Transition Temperature versus Relative Humidity

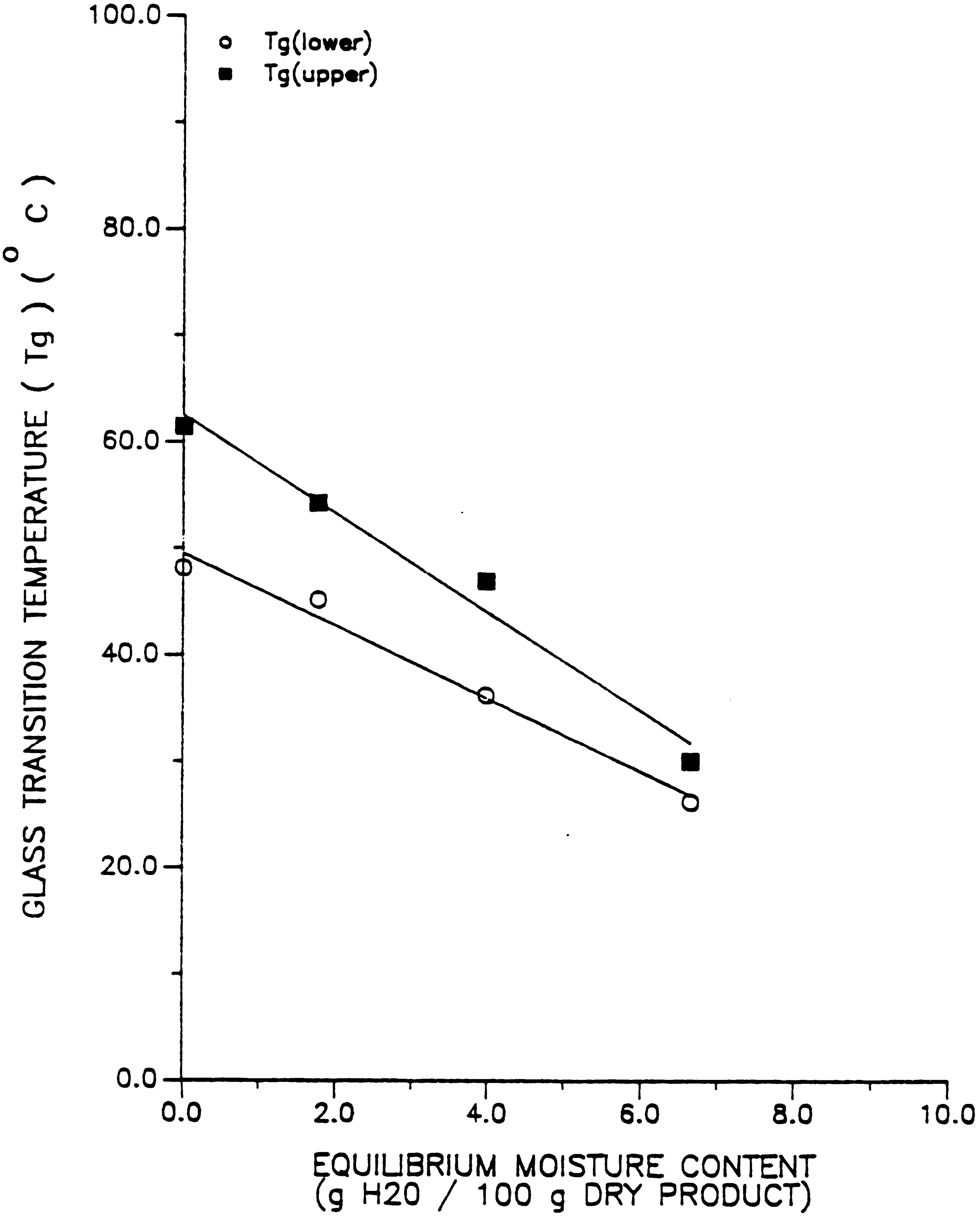

Figure 12. Plot of Glass Transition Temperature versus Equilibrium Moisture Content

were kept at 23 °C. However the toluene effects on the EVAL samples were not considered in the DSC analysis. It is possible that the toluene would lower the Tg further. Hence, if the temperature of the permeation test rise above the glass transition temperature, permeation breakthrough is likely. This raising of the permeation test temperature above the Tg would explain the phenomena of permeation at 75 and 85 %RH and no permeation detected at 50 %RH.

From Figures 11 and 12, it can be seen that a linear relationship exists between the glass transition temperature and increasing relative humidity. The reduction in Tg with increased moisture sorbed can also be related to the plasticization of the EVAL film by water sorbed. The degree of plasticization is related to the Tg. As the plasticization effect increases in the film due to the increase of absorbed moisture, the glass transition temperature decreases. This result provides supportive evidence for the proposed mechanism by Liu (1986).

Only one sample, 0 %RH, was tested with the TMA and the result is shown in Figure 13. The result of the TMA run, as shown in Figure 13, was inconclusive. The sample expanded outward rather than upwards against the probe. Thus, the probe depressed into the expanding film with increasing temperature and the measured dimensional change was negative.

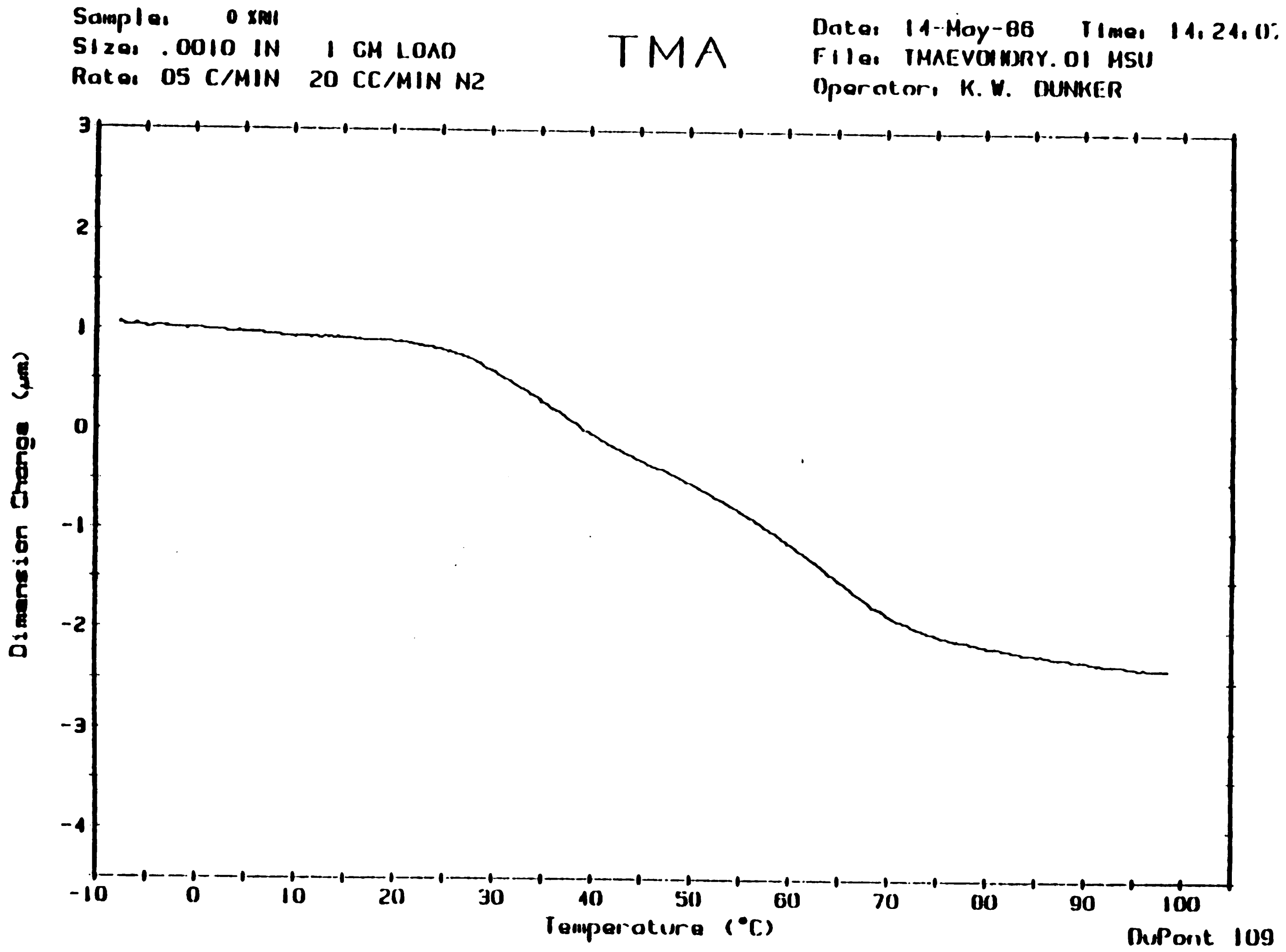

Figure 13. Plot of One Dimensional Change in Volume versus Temperature at 0 Percent Relative Humidity

Stress Relaxation

The effects of relative humidity and toluene vapor permeation on the stress relaxation of the EVAL samples, as measured by the Instron tensile tester, are shown in Figures 14, 15 and 16 for the strain rates of 0.025, 0.05, and 0.25 min^{-1} respectively. In all cases the stress relaxation properties of the polymer films were determined immediately following removal of the test film from the permeability cell. The relaxation time (τ) for the repetitive film samples, were obtained with a best fit linear regression of the Maxwell model equation

$$E(t) = E_o \exp(-t/\tau) \qquad (29)$$

where E_o is the initial load at which relaxation begins, E(t) is the relaxation load measured with time, t is the real time. The results are listed in Table 5 and presented graphically in Figure 17.

From Figures 14, 15, and 16, there appears to be a trend in the stress relaxation as a function of relative humidity. As shown, the dry sample relaxes at a slower rate than that of the humidified samples and as the humidity to which the samples were conditioned increases, the samples relax at a faster rate. Assuming the trend is

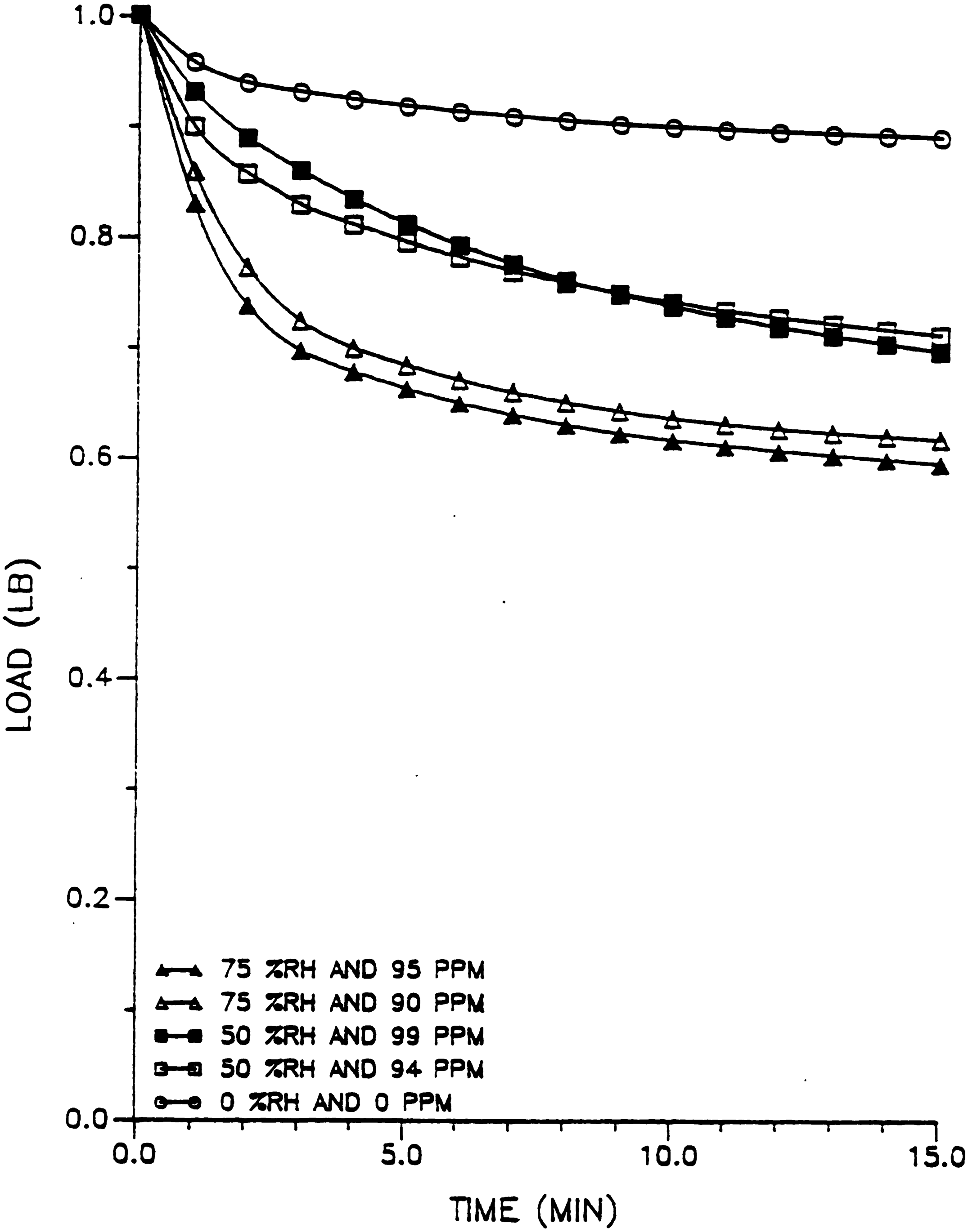

Figure 14. Plot of Stress Relaxation versus Time for Dry and Test EVAL Film Samples at 0.025 min^{-1} Strain Rate

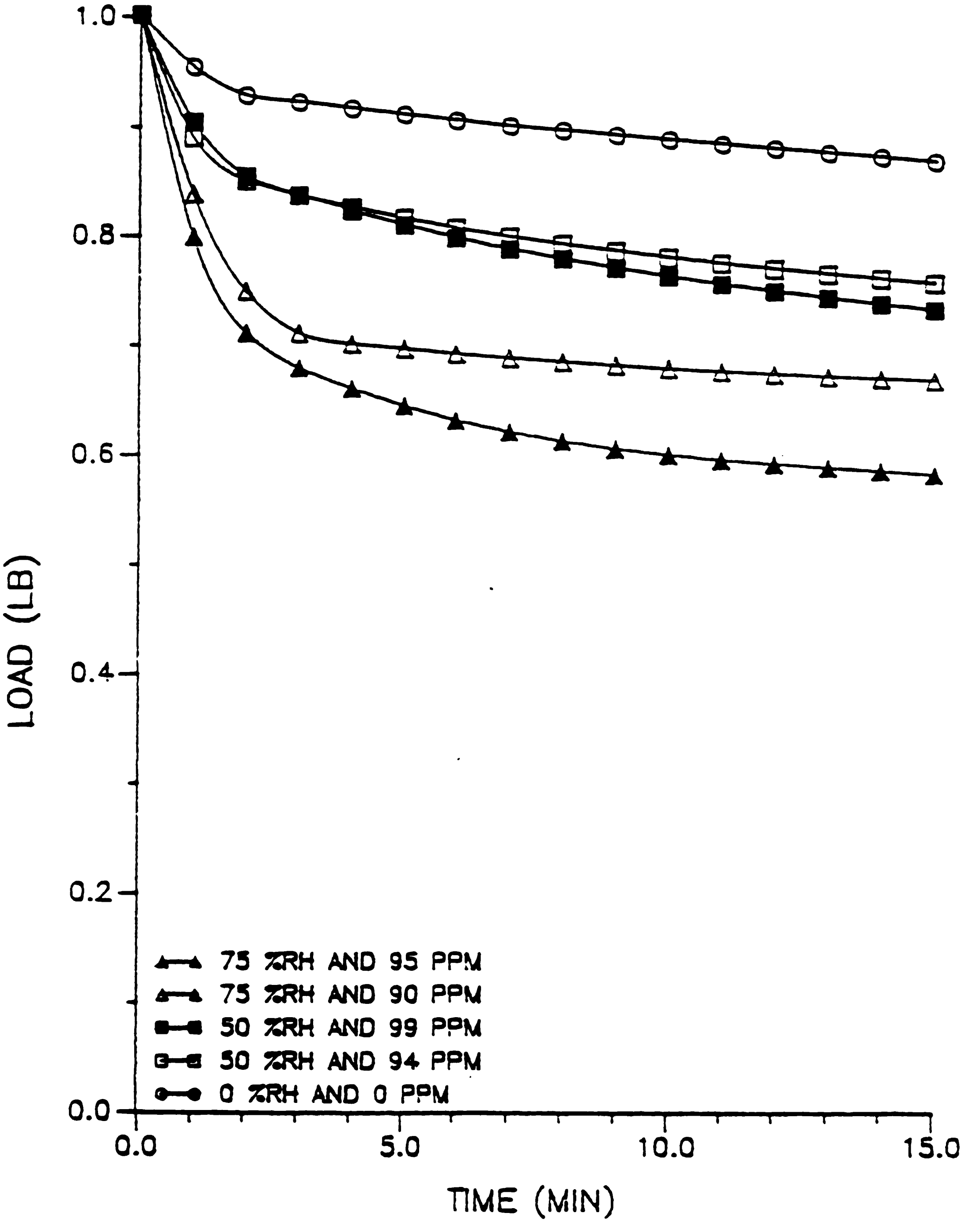

Figure 15. Plot of Stress Relaxation versus Time for Dry and Test EVAL Film Samples at 0.05 min^{-1} Strain Rate

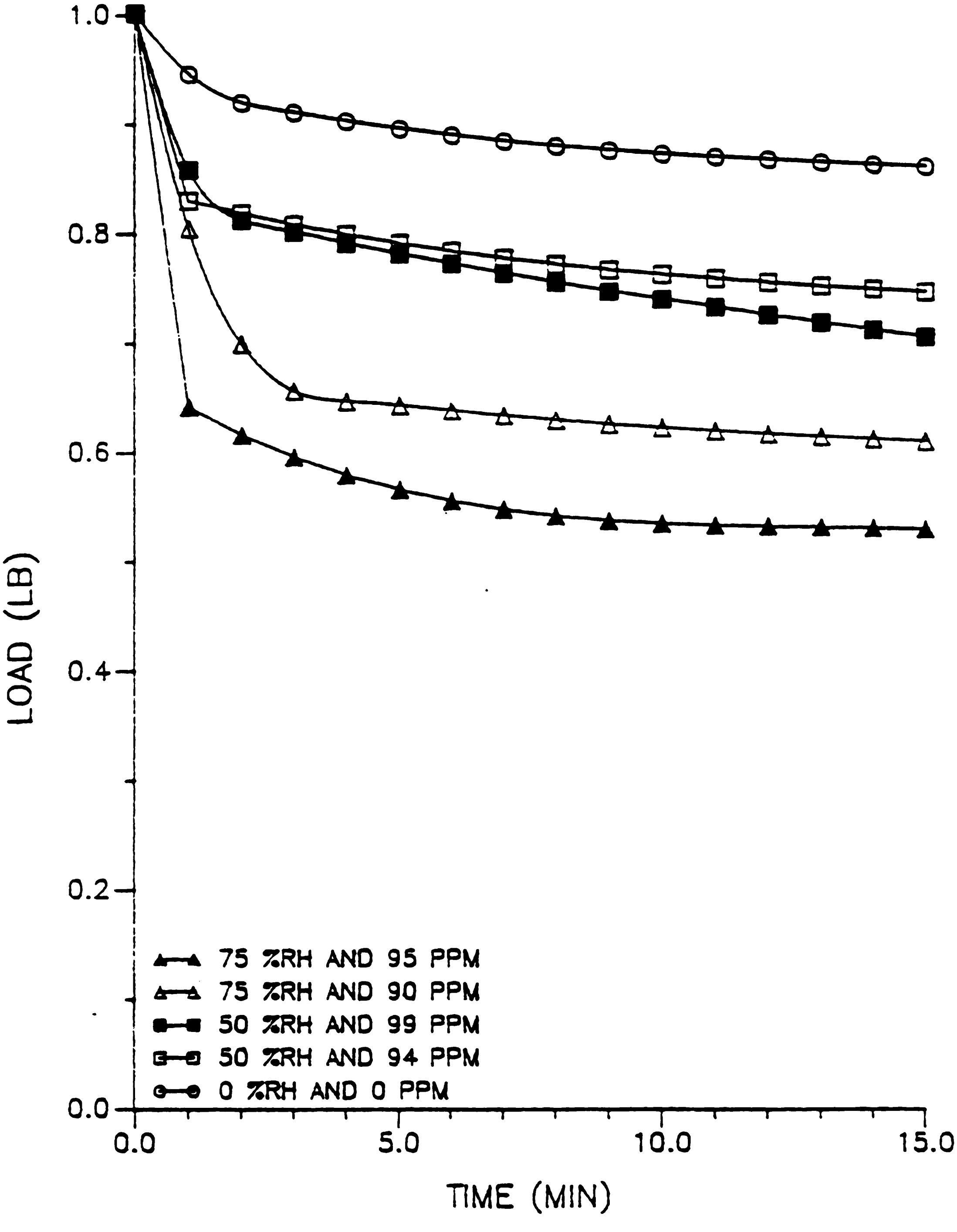

Figure 16. Plot of Stress Relaxation versus Time for Dry and Test EVAL Film Samples at 0.25 min^{-1} Strain Rate

Table 5. Effects of Relative Humidity and Toluene Vapor on Relaxation Time (τ)

%RH	Toluene Conc. (ppm) (w/v)	Strain Rate (min)	(τ) (min)	(± error)
0	0	0.025	366	9
		0.05	199	1
		0.25	217	2
50	99	0.025	71	1
		0.05	79	1
		0.25	94	1
	94	0.025	109	1
		0.05	143	1
		0.25	177	1
75	95	0.025	97	2
		0.05	83	3
		0.25	114	3
	90	0.025	86	2
		0.05	115	1
		0.25	124	4
87.5	99	0.025	104	2
		0.05	133	3
		0.25	184	2
	91	0.025	144	1
		0.05	175	4
		0.25	99	7

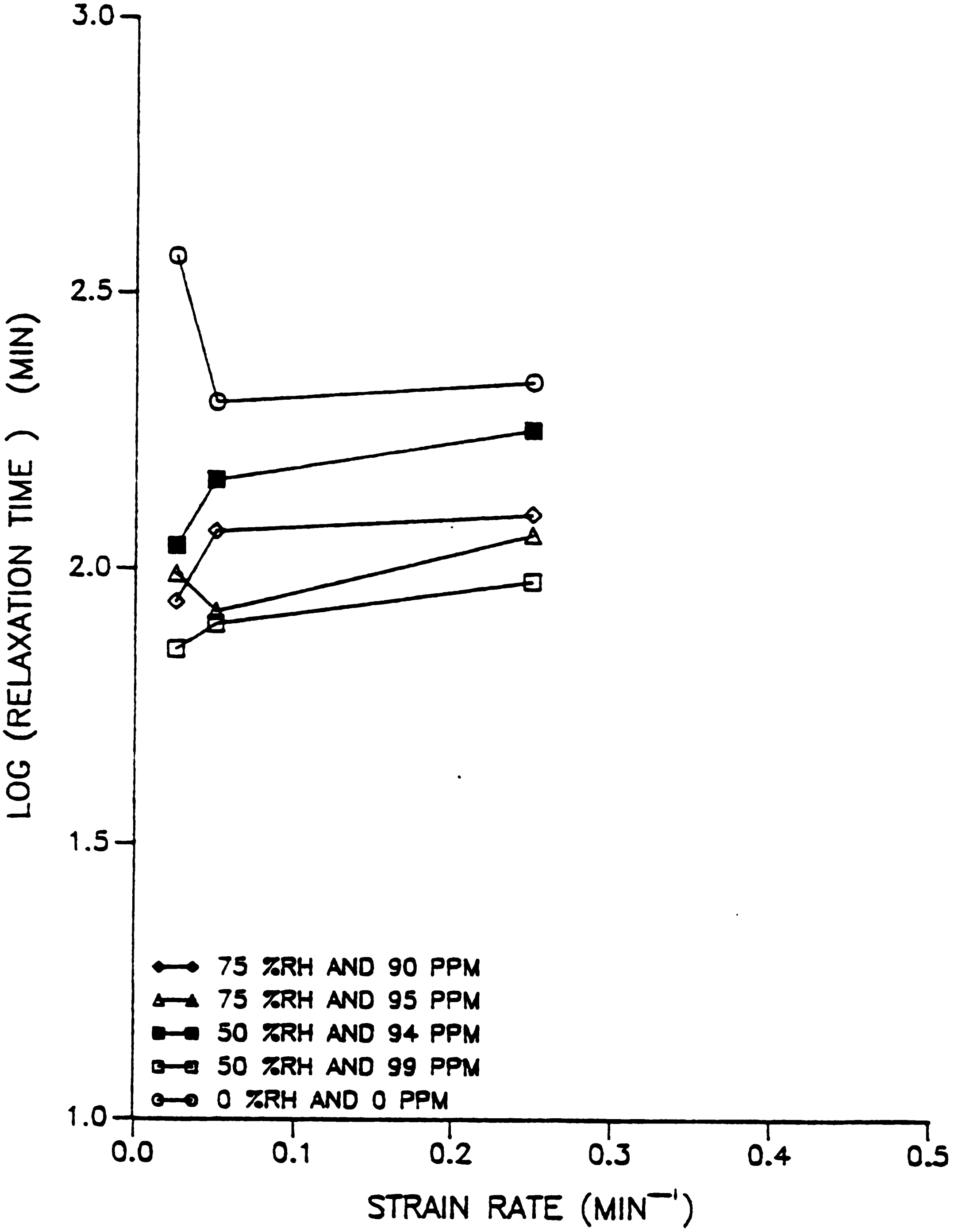

Figure 17. Plot of Log (Relaxation Time) versus Strain Rate at 0.025, 0.05, and 0.25 min^{-1}

correct, Samples 2 and 3, 87.5 % RH, gave anomalous results, which are not totally understood. However, a possible explanation for this inconsistency may be due to the Instron equipment malfunctioning during that period of operation. Thus the analysis was limited to film samples conditioned to 0, 50, and 75 % RH.

From Table 5, the results showed that the relaxation time at 0 %RH is higher than the relaxation times of the humidified samples. This result is due to sorbed water vapor plasticizing the film matrix, thereby increasing segmental chain mobility and reducing the relaxation time. Comparisons of the relaxation times at each relative humidity with varying vapor concentration showed a trend of strain softening as the vapor concentration of toluene is increased. At 50 %RH and strain rate of 0.025 min^{-1}, the relaxation time at 94 ppm is higher than the relaxation time at 99 ppm. This trend is repeated even at strain rate of 0.05 and 0.25 min^{-1}. At 75 % RH, the same trend is seen. A possible explanation to this phenomena of strain softening is that the water vapor, at each relative humidity, initially plasticizes the samples to an equilibrated state and then, toluene vapor interacting with the equilibrated samples further increases the "softening".

Further comparisons between the relaxation times at 50 and 75 %RH at a fixed vapor concentration of 94 - 95 ppm showed that the relaxation time at 75 %RH is lower than that of the 50 %RH. This result shows the effect of sorbed water vapor on the EVAL samples. As the relative humidity (water sorbed) is increased at a fixed vapor concentration, the relaxation time of the film sample decreases. Since EVAL is a hydrophilic semi-crystalline copolymer, the amount of water sorbed would have an effect on its polymer matrix. The greater the amount sorbed, the greater the effects (i.e. plasticization) would be. At 50 %RH, the amount of water sorbed enhances the plasticization effect and the toluene sorbed further increases the effect, which can be seen from the results of the relaxation times. However, the amount of water sorbed and the enhanced plasticization by toluene was insufficient to modify the barrier properties of the film to the extent that a measureable level of permeation could be detected. However, at 75 %RH, permeation was detected even at a similar toluene vapor concentration. Thus, the amount of water sorbed appears to play a greater role in the plasticization effect than the amount of toluene sorbed.

The relaxation times from Table 5 were further analyzed to determine the fractional free volume of the test film, and are tabulated in Table 6. The equation applied in determining the fractional free volume was Equation 20 with the Poisson's ratio as 0.33 (a common value for semi-crystalline copolymer film, Krevelen 1972). The equation can be simplified and rearranged to solve for the fractional free volume:

$$A = 4*[1/(0.34*\epsilon)]*[1/\ln a_{\epsilon}] \qquad (30)$$

$$B = 2*[1/(0.34*\epsilon)]$$

$$f_o = [-1 \pm (1-A)]/B$$

The strain shift factor is determined by calculating the ratio of relaxation times at each strain rate. As shown in Table 6, the fractional free volume increased from strain rate of 0.025 to 0.25 min^{-1} at each condition and is presented graphically in Figure 18. However, in comparing the fractional free volume at each strain rate, the changes are minimal and can be accounted for by the error in strain.

Table 6. Determination of Fractional Free Volume at Strain Rates of 0.025, 0.05, and 0.25 in/min

Strain Rate $(\text{min})^{-1}$	Strain (ϵ)	Conditions $T(2)/T(1)$	Shift Factor (a_{ϵ})	Fractional Free Volume ($f_{0\epsilon}$)
0.025	0.01324	50%,99ppm/0%,0ppm	0.19399	0.050197
		50%,94ppm/0%,0ppm	0.29781	0.058761
		75%,95ppm/0%,0ppm	0.26503	0.056024
		75%,90ppm/0%,0ppm	0.23497	0.058056
0.05	0.01106	same as above	0.39698	0.061936
			0.71859	0.104792
			0.41709	0.063713
			0.57789	0.080937
0.25	0.01479	same as above	0.43318	0.075059
			0.81567	0.154613
			0.52535	0.085911
			0.57143	0.092317

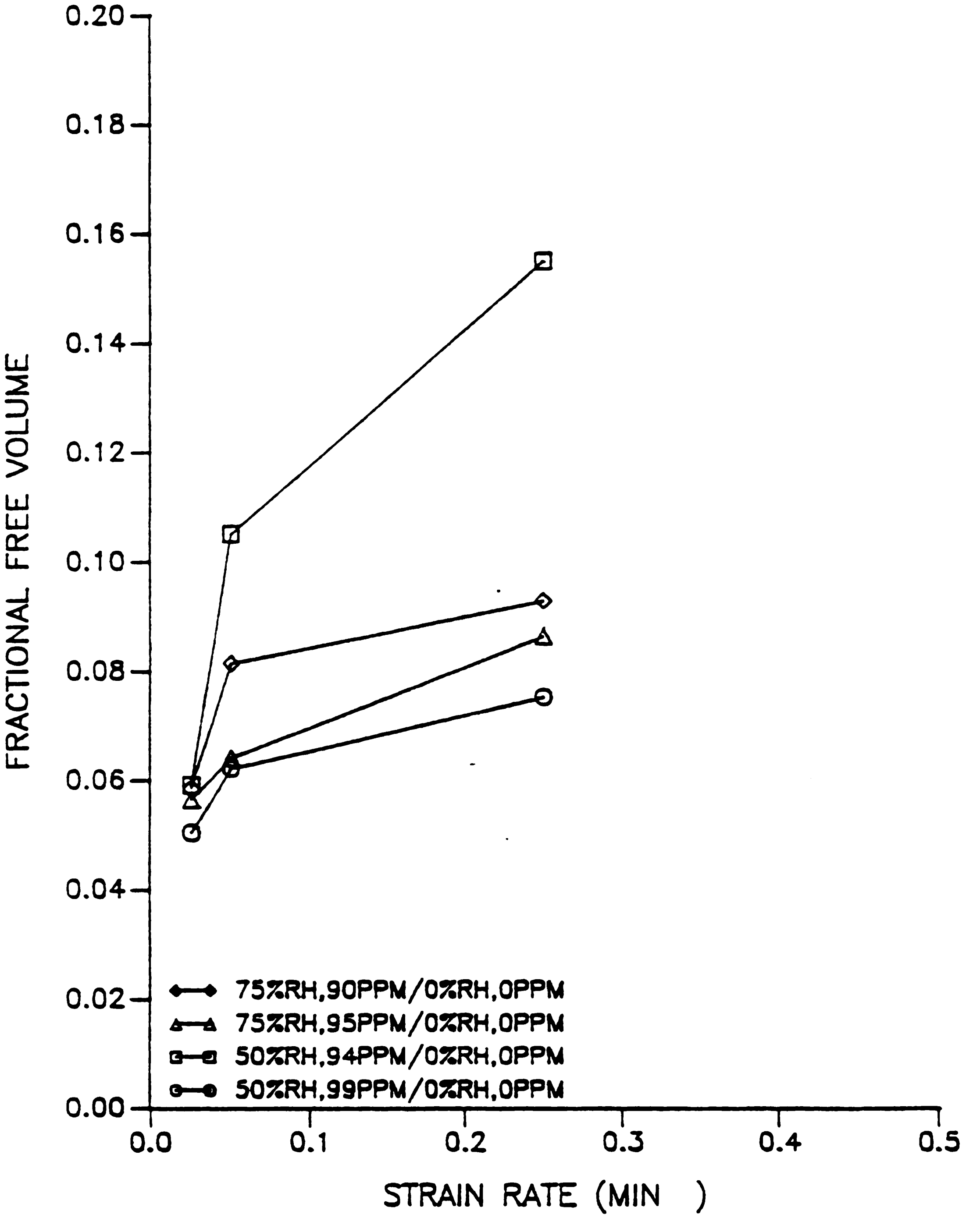

Figure 18. Plot of Fractional Free Volume versus Strain Rate at 0.025, 0.05, and 0.25 min^{-1}

CONCLUSION

These studies were designed to develop a better understanding of the effect of water vapor on the permeation of toluene through a high barrier copolymer film, EVAL. Physical and mechanical properties (i.e. Tg and relaxation time respectively) were related to the permeation of toluene at varying relative humidity. It was found that water vapor exhibits strong interactive effects with the barrier structure, and that the diffusion of toluene vapor through the structure is dependent on the equilibrium moisture content in the film.

DSC analysis of the glass transition temperature of EVAL showed a linearly decreasing temperature with increasing relative humidity (i.e. water sorbed). This observation can be related to the plasticization effect of the EVAL film by the water sorbed, which acts as a plasticizer and causes a reduction of the interchain hydrogen bonding of the polymer matrix. This reduction of hydrogen bonding will result in the increase in segmental motion of the polymer chain. It was also found that if the Tg of the test film falls below or near the test temperature, permeation breakthrough is likely.

Analysis of the relaxation times showed the same trend, that is, a decrease in relaxation time with increasing relative humidity. This observation provided supportive evidence of the plasticization effect of the EVAL film by the water sorbed. As the film approaches the transition from glassy to rubbery states, the relaxation time is found to decrease strongly.

RECOMMENDATION

The effects of organic and water vapor sorbed on EVAL have been studied over a range of 87 to 99 ppm and from 0 to 87.5 %RH. The results showed that there exists a relative humidity threshold, 50 to 75 %RH, where a breakthrough of the organic vapor occured. At 50 %RH, no permeation was detected even at a toluene concentration of 99 ppm. The Tg of the film was well above the test temperature. However, at 75 %RH, permeation was detected at a measureable level at 89 ppm and the Tg of the film was near to the test temperature. Therefore, depending upon the relative humidity, there exists also a toluene concentration threshold which would permit permeation through EVAL. It is recommended that the effects of organic vapor over the range of 50 to 75 %RH should be studied to determine the relative humidity and concentration threshold. The breakthrough point should then be related to the Tg of the test film. The equipment recommended for this study is the DSC and the permeation system (as described in the materials and procedure section).

The relation between physical and mechanical properties is important in the overall study of barrier properties of polymer films. A more extensive study than the one presented in this study is required to relate the physical properties (i.e. permeation) with mechanical properties (i.e. relaxation times and fractional free volume). The permeation data may be obtained from a permeation system. The mechanical properties are best studied at one strain rate, preferably in the high range, and with only one permeant, perhaps toluene, at varying concentration. The equipment recommended for the mechanical study is either a computerized Instron with a capability of measuring sensitively low loads or the Dynamic Mechanic Analyzer, DMA.

BIBLIOGRAPHY

Alfrey, T., "Mechanical Behavior of High Polymers," Interscience, 533 (1948).

Alfrey, T., Gurnee, E.F., Lloyd, W.G., "Diffusion in Glassy Polymers," J. Polymer Science C12, 249 (1966).

American National Standards (ANS, 1979).

ASTM Designation E104-54, Standard Method of Test for Saturated Salt Solutions, Annual Book of ASTM Standards, American Society for Testing Materials, Library of Congress.

Baner, A.L., "Diffusion and Solubility of Toluene in Polymeric Films," School of Packaging, Michigan State University (1985).

Barrer, R.M., "Permeation, Diffusion and Solution of Gases in Organic Polymers," Trans. Faraday Soc. 35, 628 (1939).

Barrer, R.M., Diffusion In and Through Solids, London, Cambridge Univ. Press (1941).

Barrie, J.A., "Water in Polymers," Diffusion in Polymers, Academic Press, London & New York (1968).

Barrie, J.A., Nunn, A., and Sheer, A., "Sorption and Diffusion of Water in Polyurethane Elastomers," Polymer Science and Technology #6, Plenum Press, New York (1974).

Choy, C.L., Leung, W.P., and Ma, T.L., "Sorption and Diffusion of Toluene in Highly Oriented Polypropylene," J. Polymer Science, Physics ed. 22, 707 (1984).

Cohen, M.H. and Turnbull, D., "Molecular Transport in Liquids and Glasses," J. Chem. Phys. 31, 1164-1169 (1959).

Combellick, W.A., Barrier Polymers, Encyclopedia of Polymer Science & Technology, 2nd. ed., Vol. 2. John Wiley & Sons, N.Y. (1985).

Crank, J. and Park, G.S., "Diffusion in High Polymers: Some Anomalies and Their Significance," Trans. Faraday Soc. 47, 1072 (1951).

DeLassus, P.T., "Transport of Unusual Molecules in Polymer Films," TAPPI Proceedings of Polymers, Laminations & Coatings Conference (1985).

Ferry, J.D., Viscoelastic Properties of Polymers, 2nd. edition, John Wiley and Sons, Inc. (1970).

Fujita, H., "Diffusion in Polymer-Diluent Systems," Fortschr. Hochpolym Forsch. 3, 1 (1961).

Fujita, H., Kishmoto, A., and Matsumoto, K., "Concentration and Temperature Dependence of Diffusion Coefficients for Systems Polymethyl Acrylate and n-Alkyl acetates," Trans. Faraday Soc. 56, 424 (1960).

Hernandez, R., "Permeation of Toluene Vapor through Glassy Poly(ethylene) Terephthlate Films," Master of Science Thesis, School of Packaging, Michigan State University (1984).

Kaufman, H.S. and Falcetta, J.J., Introduction to Polymer Science and Technology : An SPE Textbook, Wiley & Sons, New York (1977).

Kovacs, A., Advance Polymer Science 3, 394 (1964).

Krevelen, V., Properties of Polymers, Correlations with Chemical Structure, 1st ed., American Elsevier Publishing Co., Inc. 1972.

Kulkarni, M.G. and Mashelkar, R.A., "A Unified Approach to Transport Phenomena in Polymeric Media - I & II," Chemical Engineering Science 38, 925-953 (1983).

Long, F.A. and Thompson, L.J., "Water Induced Acceleration of the Diffusion of Organic Vapors," J. Polymer Science 14, 321 (1954).

Liu, K., "Evaluation of the Effect of Relative Humidity on the Permeation of Toluene Vapor Through Barrier Films," Master of Science thesis, School of Packaging, Michigan State University (1986).

Michaels, A.S., Vieth, W.R., Barrie, J.A., "Solution of Gases in Polyethylene Terephthalate," J. Appl. Physics 34, 1-12 (1963).

Pasternak, R.A., Schimscheimer, J.F., and Heller, J., "A Dynamic Approach to Diffusion and Permeation Measurements," J. Polymer Sci., Part A-2, 8, 467 (1970).

Peterlin, A., "Steady State Transport Phenomena in Non-Ideal Permeant-Polymer Systems," Polymer Science and Technology, Plenum Press, New York (1974).

Petropoulos, J.H., "Interpretation of Anomalous Sorption Kinetics in Polymer-Penetrant Systems in Terms of a Time-Dependent Solubility Coefficient," J. Polymer Science, Physics edition 22, 1885-1900 (1984).

Rogers, C. , Meyer, J.A., Stannett, V., "Studies in the Gas and Vapor Permeability of Plastic Films and Coated Papers Part I and II," TAPPI 39, No. 11 (1956).

Rodriguez, F., Principles of Polymer Systems, 2nd. edition, McGraw Hill, Washington, New York, and London (1982).

Simha, R. and Boyer, R.F., "On a General Relation Involving the Glass Temperature and Coefficients of Expansion of Polymers," J. Chem. Phys., 37, 1003 (1962).

Schwarzl, F. and Staverman, A.J., Appl. Sci. Research A4,127 (1953).

Salame, M., "Prediction of Gas Barrier Properties of High Polymers," Second International Ryder Conference, "Packaging Innovations" Dec. 3-5 (1984).

Smith, T.L., "Nonlinear Viscoelastic Response of Amorphous Elastomers to Constant Strain Rates," Trans. Soc. Rheology 6,61 (1962).

Stern, S.A. and Fang, S.M., "Effect of Pressure on Gas Permeability Coefficients," J. of Polymer Science, A-2. 10, 201 (1972).

Tobolsky, A.V., "Stress Relaxation Studies of the Viscoelastic Properties of Polymers," J. Applied Physics 27,673 (1956).

Tobolsky, A.V. and Murakami, K., "Existence of a Sharply Defined Maximum Relaxation Time for Monodisperse Polystyrene," J. Polymer Sci. 40,443 (1959).

Vrentas, J.S., Duda, J.L. and Ling, H.C., "Free Volume Theories for Self-Diffusion in Polymer-Solvent Systems," J. Polymer Science, Physics ed. 23, 275 (1985).

Wachtel, J.A., Tsai, B.C. and Farrell, C.J., "Retorted EVOH Multilayer Cans With Excellent Oxygen Barrier Properties," Second International Ryder Conference on Packaging Innovations, Dec. 3-5, 1984.

Ziegel, K.D., Frensdorff, H.K., and Blair, D.E., "Measurement of Hydrogen Isotope Transport in Poly (Vinyl Fluoride) Films by the Permeation-Rate Method," J. Polym. Sci., Part A-2, 7, 809 (1969).

Zoebel, M.G.R., "Measurement of Odour Permeability of Polypropylene Packaging Films At Low Odourant Levels," Polymer Testing, 33, 133 (1982).